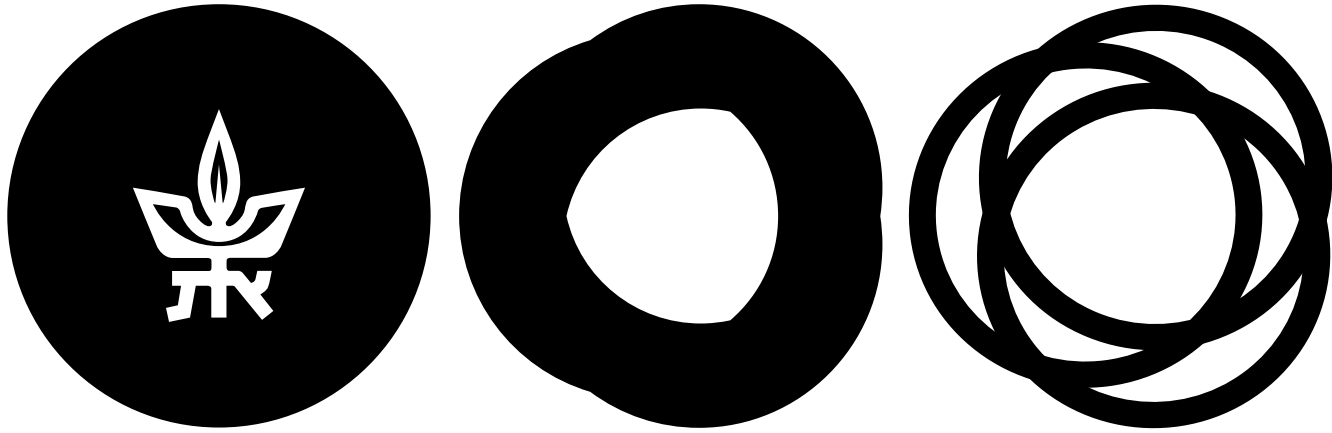


Searches for additional Higgs bosons in ATLAS



Luis Pascual Domínguez
On behalf of the ATLAS Collaboration

TEL AVIV אוניברסיטת תל אביב
UNIVERSITY תל אביב

Pheno 2022
Pittsburgh
9-11th May

Introduction

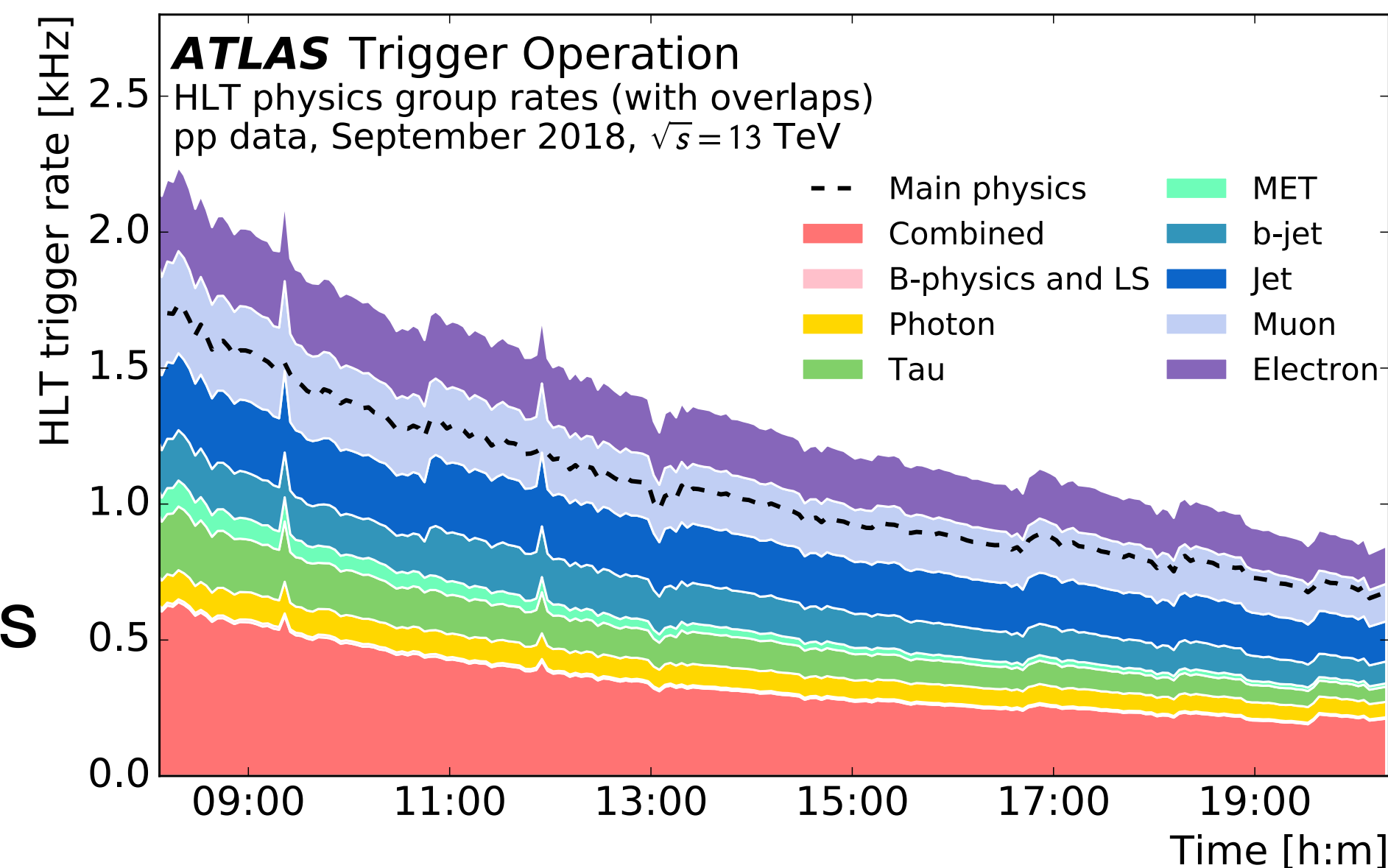
Many popular models within the community include additional fields to motivate searches for new phenomena:

- Extensions of the Higgs sector predicted in many BSM theories: Higgs doublets or triplets, composite Higgs,...
- New Physics fields weakly coupled to the SM (e.g. with axion-like particles or SUSY)

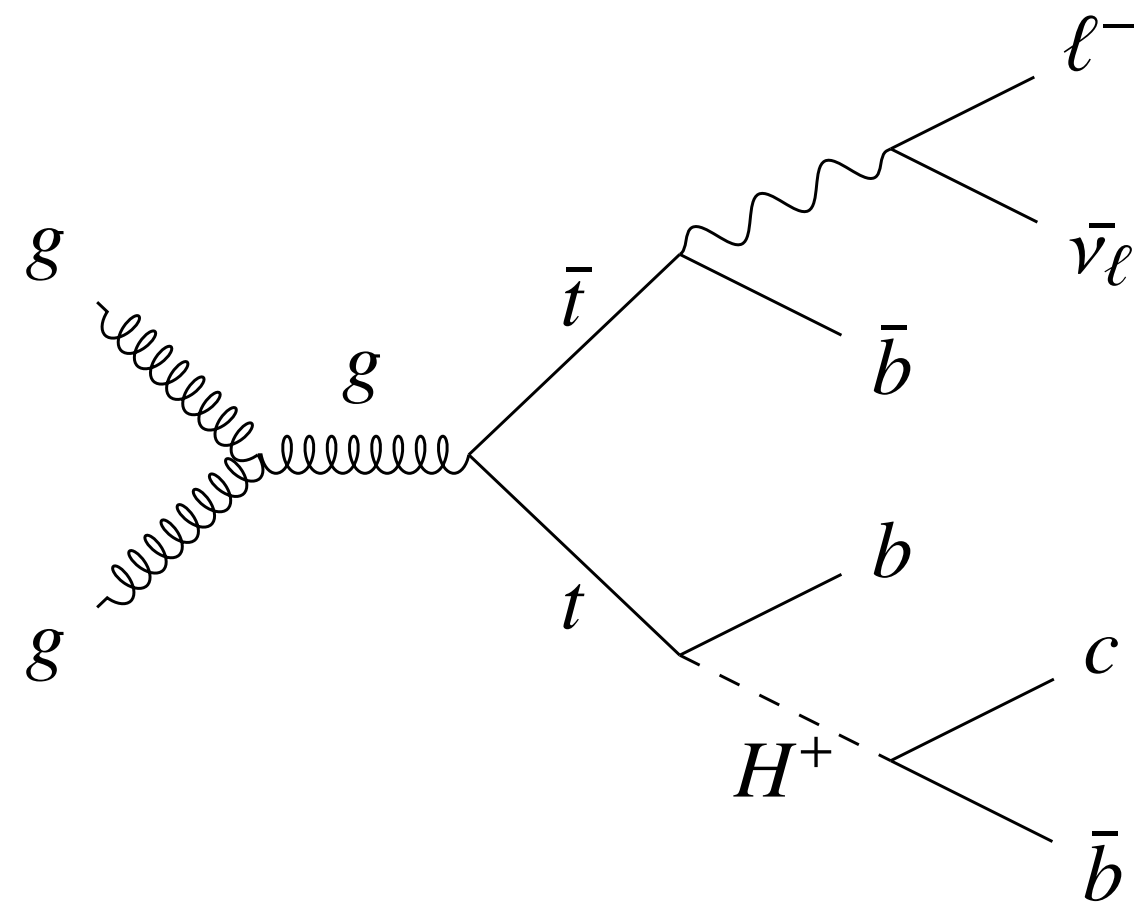
Most of these searches require leptons or photons in the final state, benefiting from the large trigger bandwidth allocated for those objects.

An overview of ATLAS searches for additional Higgs bosons is presented.

- Full Run 2 pp collision data at $\sqrt{s} = 13$ TeV used in all results shown here.



$H^\pm \rightarrow cb$



Search for charged Higgs bosons $H^\pm \rightarrow cb$ produced in top quark decays

- Motivated in non-minimal SM extensions (e.g. 3HDM)

Large jet multiplicity events (>4 jets, with > 3b-tagged) with an additional e/ μ for triggering.

Mass-parametrised Neural Networks (NN) [[Eur. Phys. J. C 76, 235](#)]

- Kinematical information from the jets, leptons and E_{miss}^T are used as input variables.

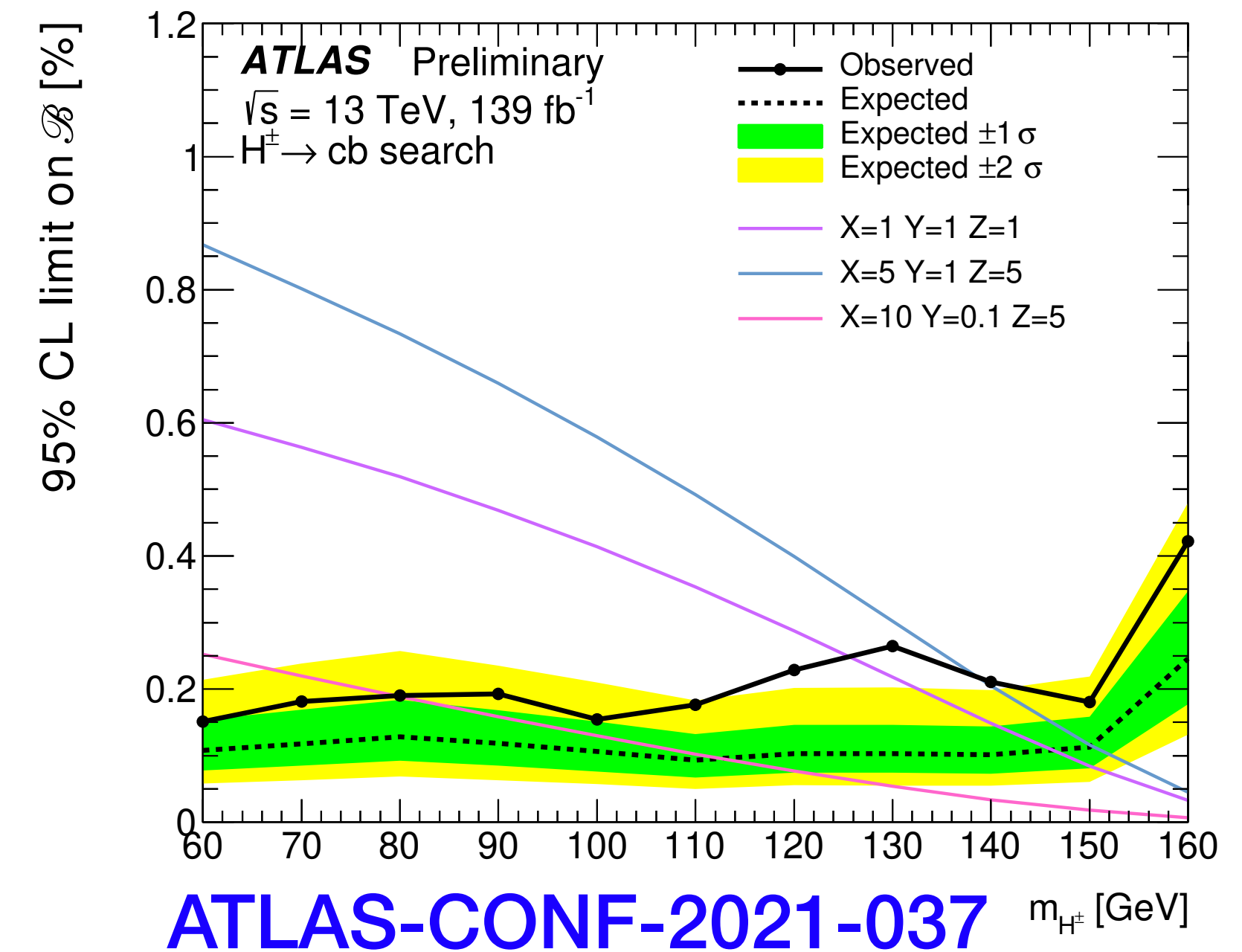
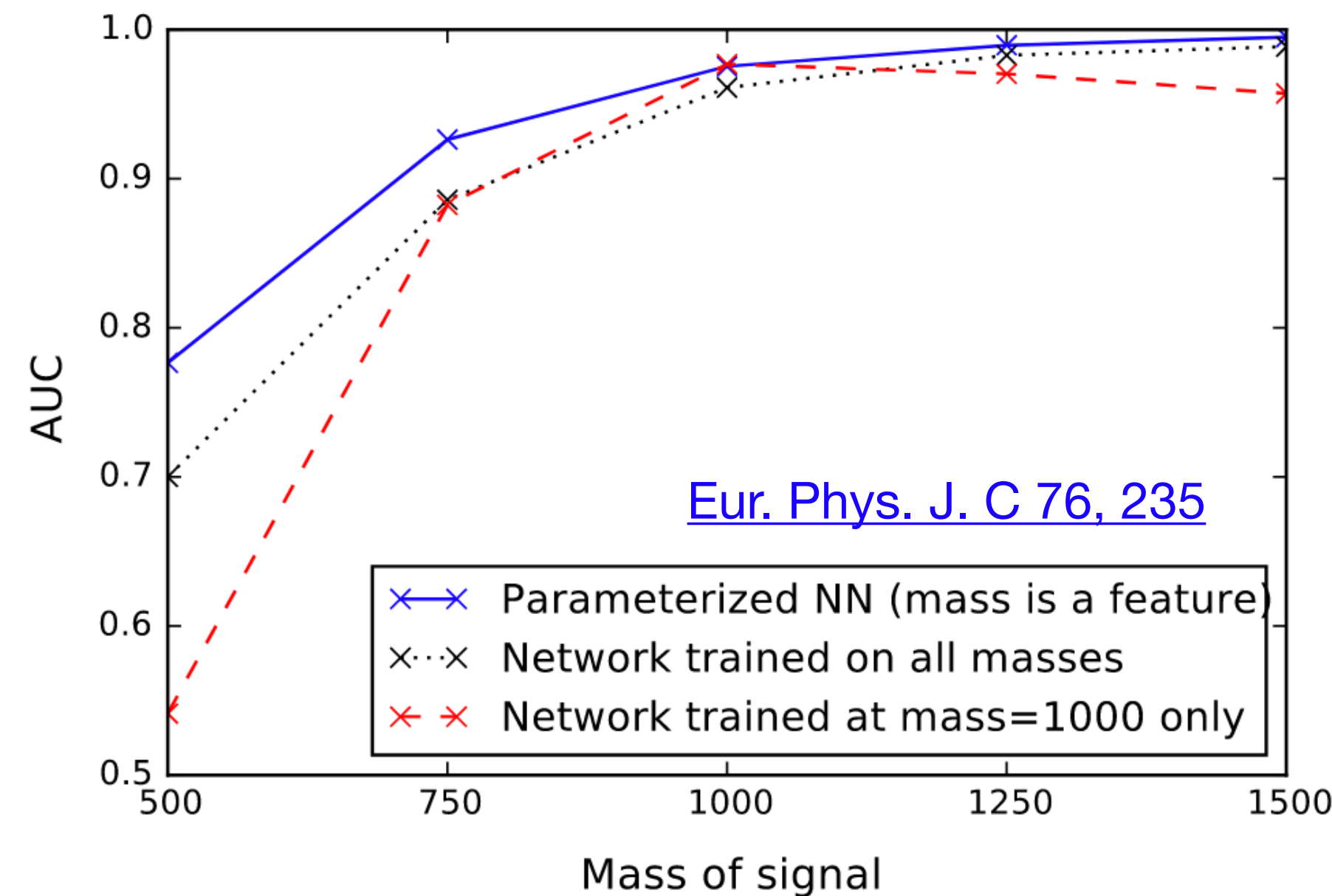
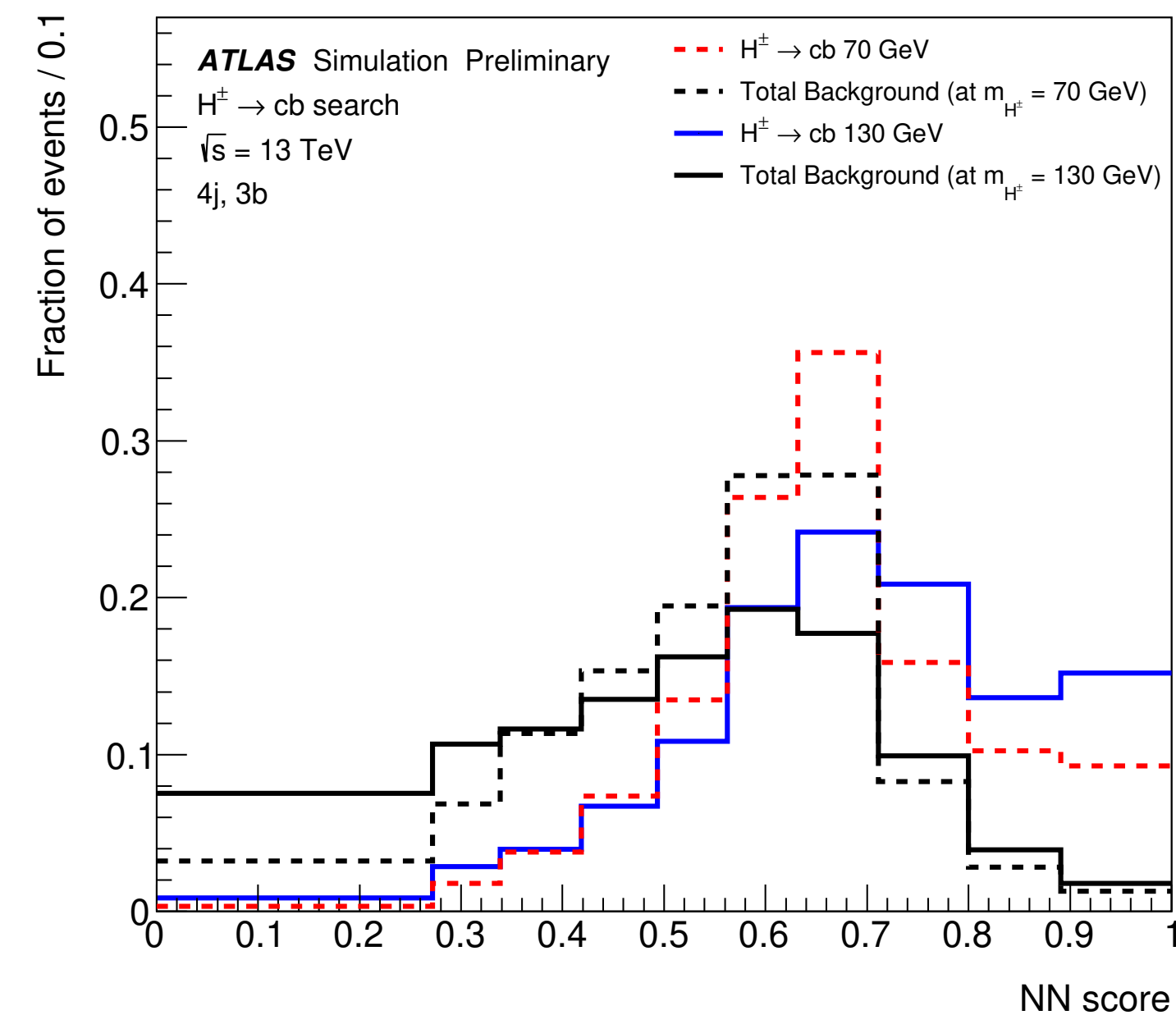
Upper limits set on $\mathcal{B}(H^\pm \rightarrow cb)$ covering masses from 60 to 160 GeV.

- Improves previous LHC result by factor x5.
- Broad excess consistent with the expected mass resolution

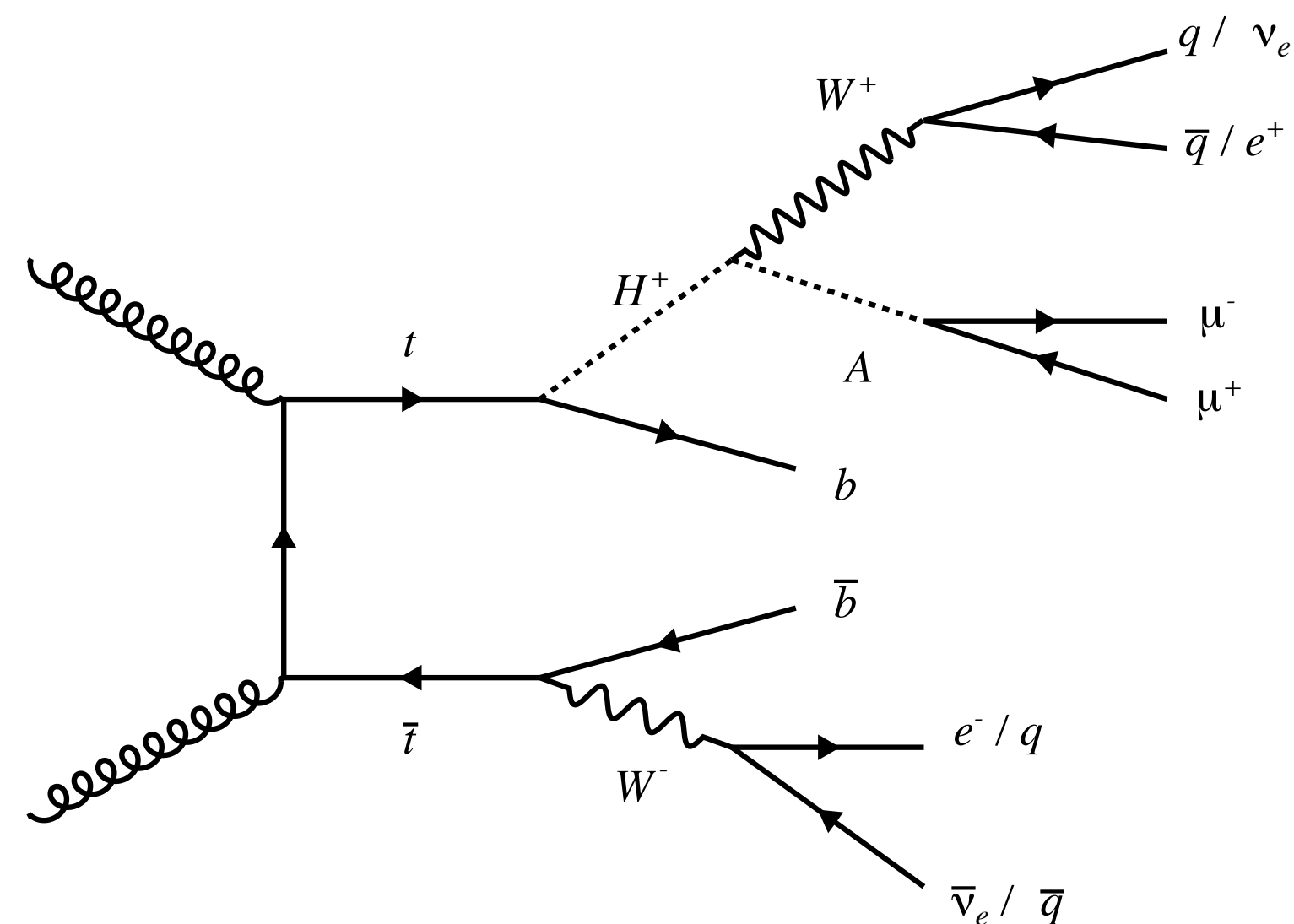
$$m_{H^\pm} = 130 \text{ GeV}$$

Local signi: 3σ

Global signi: 1.6σ



$$H^\pm \rightarrow W^\pm A, A \rightarrow \mu\mu$$



Search for a charged Higgs boson H^\pm decaying to a pseudoscalar A and a W^\pm produced in association with a top quark.

- $\mu\mu e$ final state easy to reconstruct.

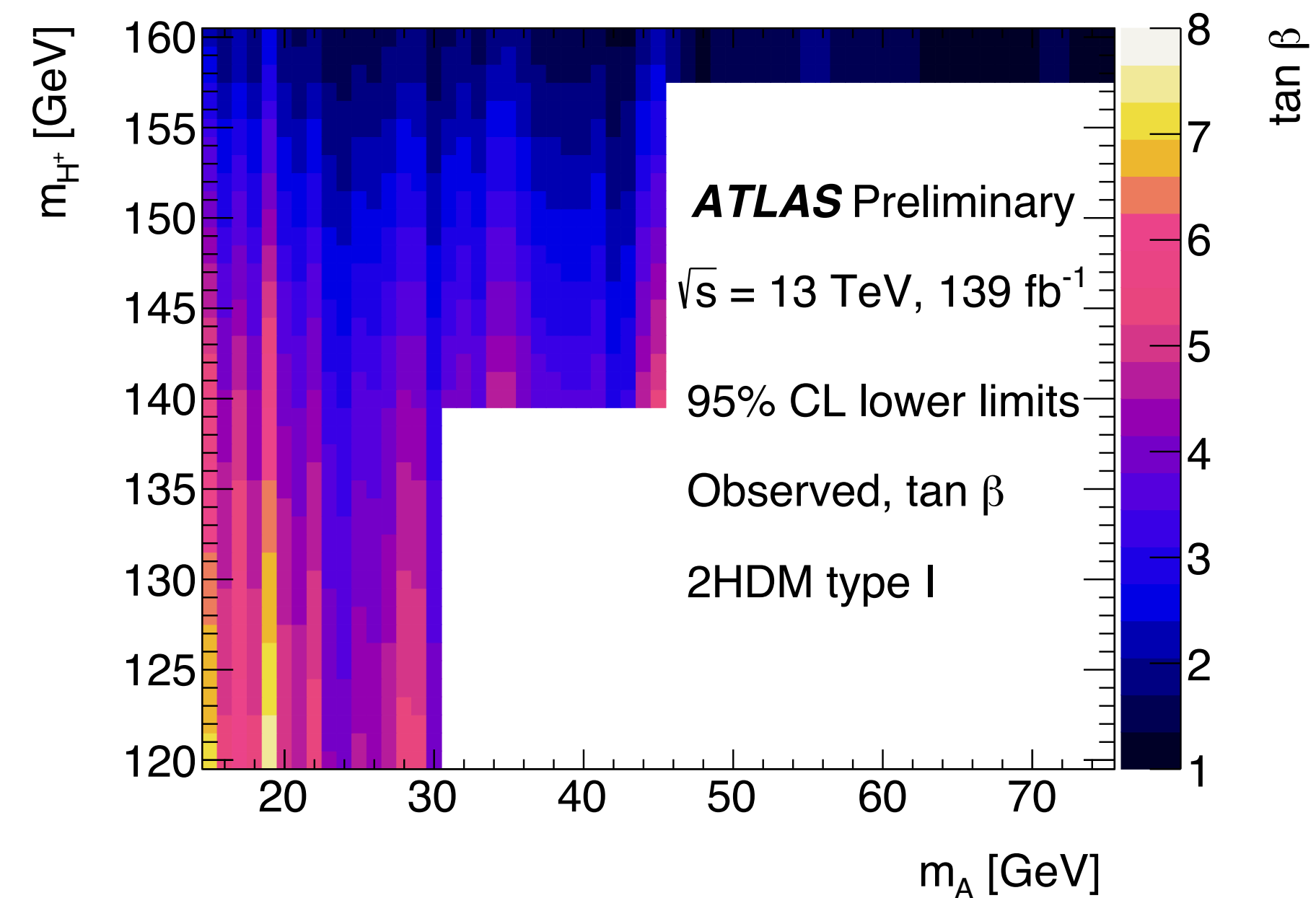
At least 3 jets (1 b-tagged) with one electron and two muons

- Muons used for triggering the events.

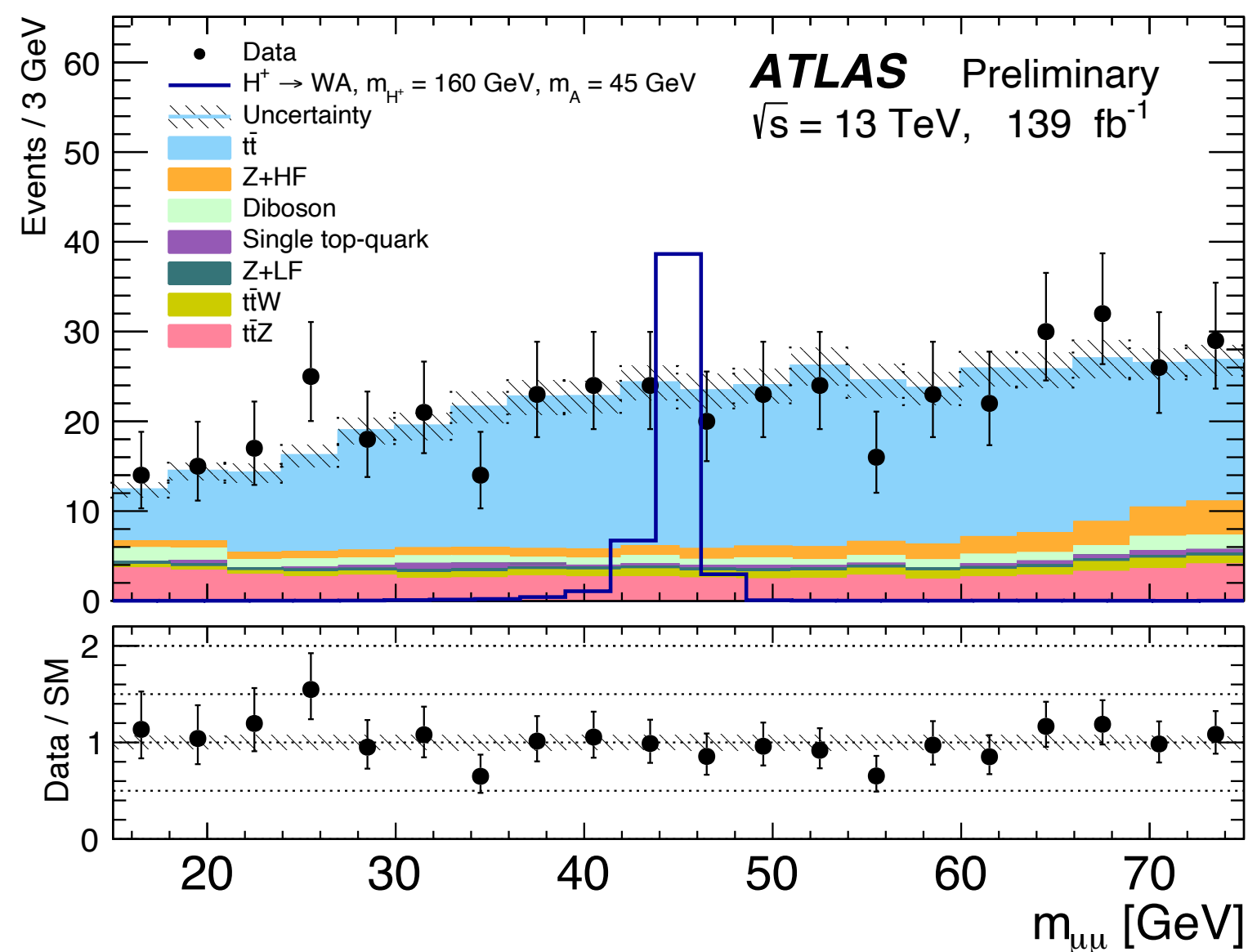
Strategy: scan the $m_{\mu\mu}$ invariant mass for event excesses.

Upper limits computed as a function of the m_A for various m_{H^\pm} hypotheses.

- First lower limit on $\tan\beta$ for a 2HDM type-I model



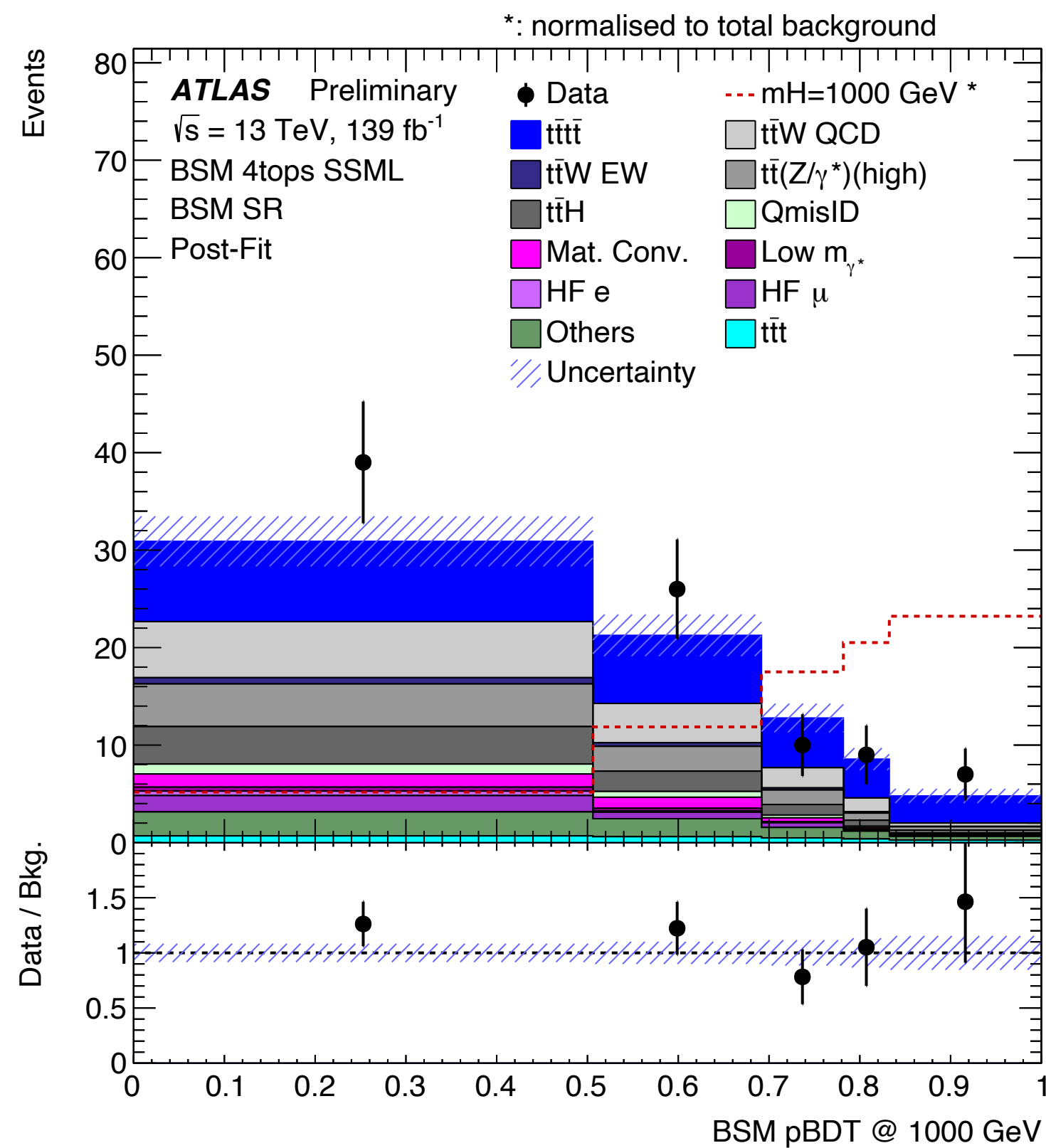
[ATLAS-CONF-2021-047](#)



$$t\bar{t}H \rightarrow t\bar{t}t\bar{t}$$

Search for heavy additional neutral Higgs-like bosons produced in association with a pair of top quarks in the $t\bar{t}t\bar{t}$ final state.

- Additional pair of top quarks motivated to reduce negative inference effects from SM $gg \rightarrow t\bar{t}$.



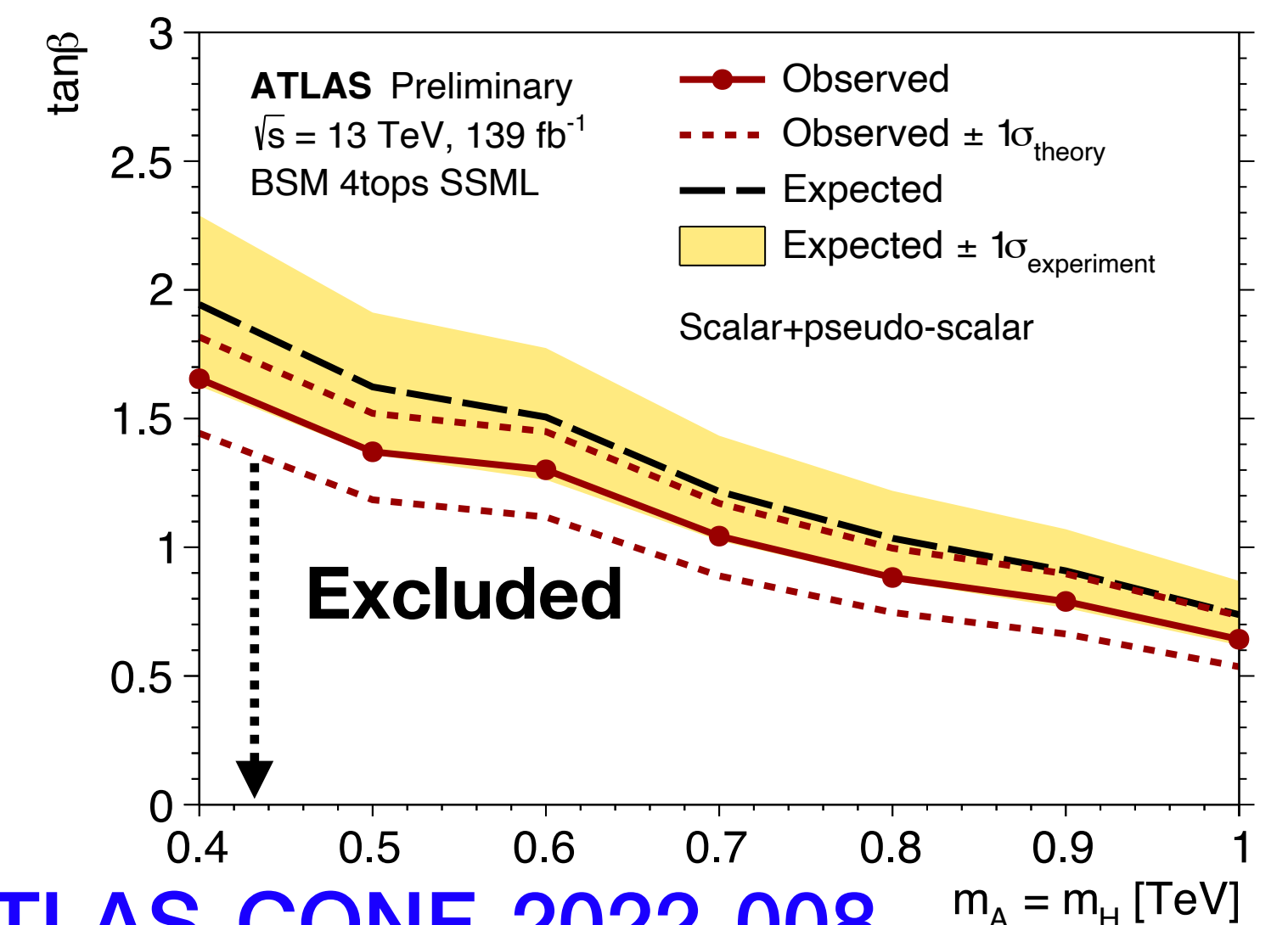
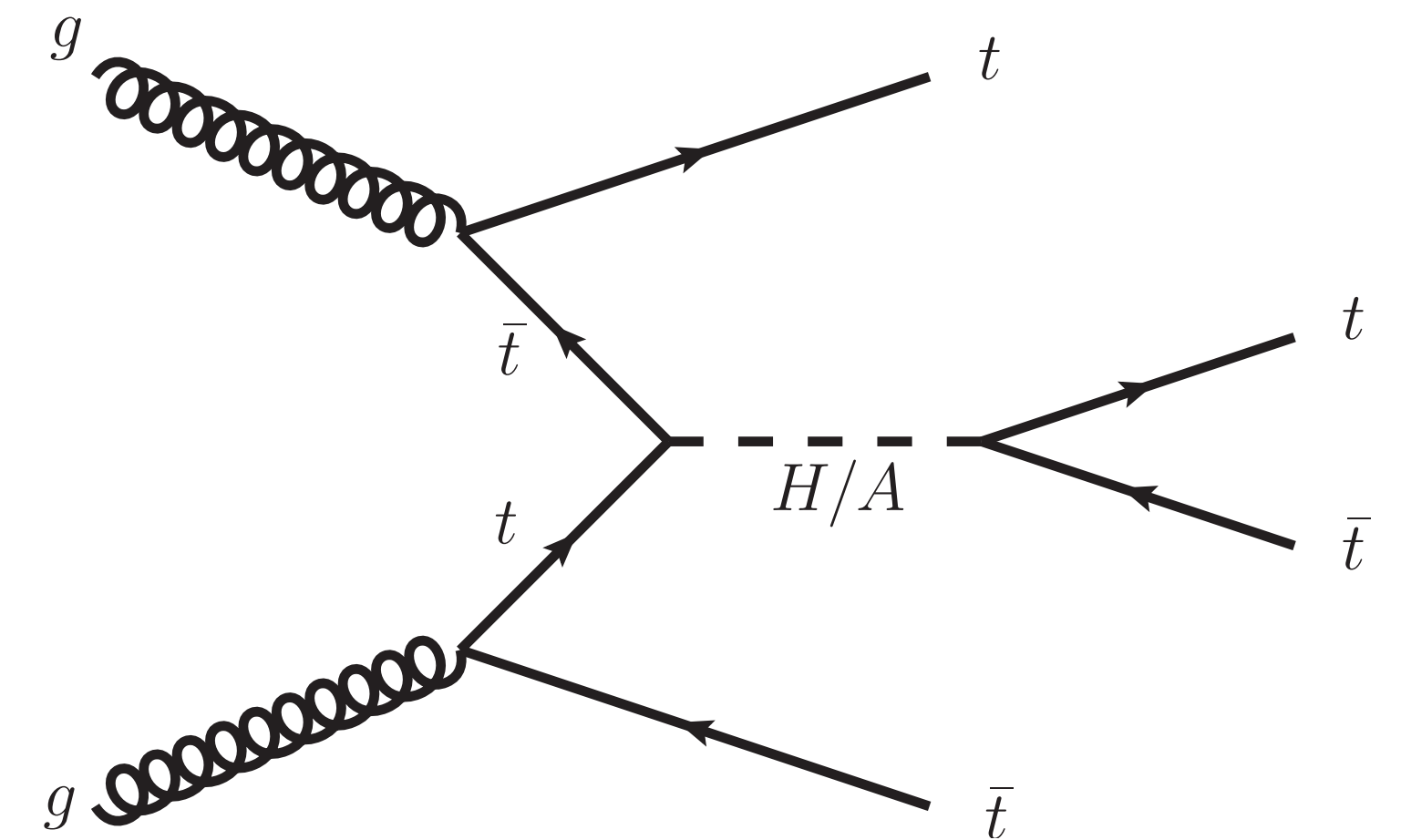
Only multi-lepton events are selected (2 same signed leptons or 3 leptons)

Analysis selection relies on sequentially applied BDTs:

- Separate SM $t\bar{t}t\bar{t}$ from other backgrounds.
- Separate BSM signal from SM $t\bar{t}t\bar{t}$

Results interpreted in the context of a type-II 2HDM

- Upper limits on production cross-section translated to limits on $\tan\beta$



[ATLAS-CONF-2022-008](#)

$$t \rightarrow qX, X \rightarrow b\bar{b} \quad (q = u, c)$$

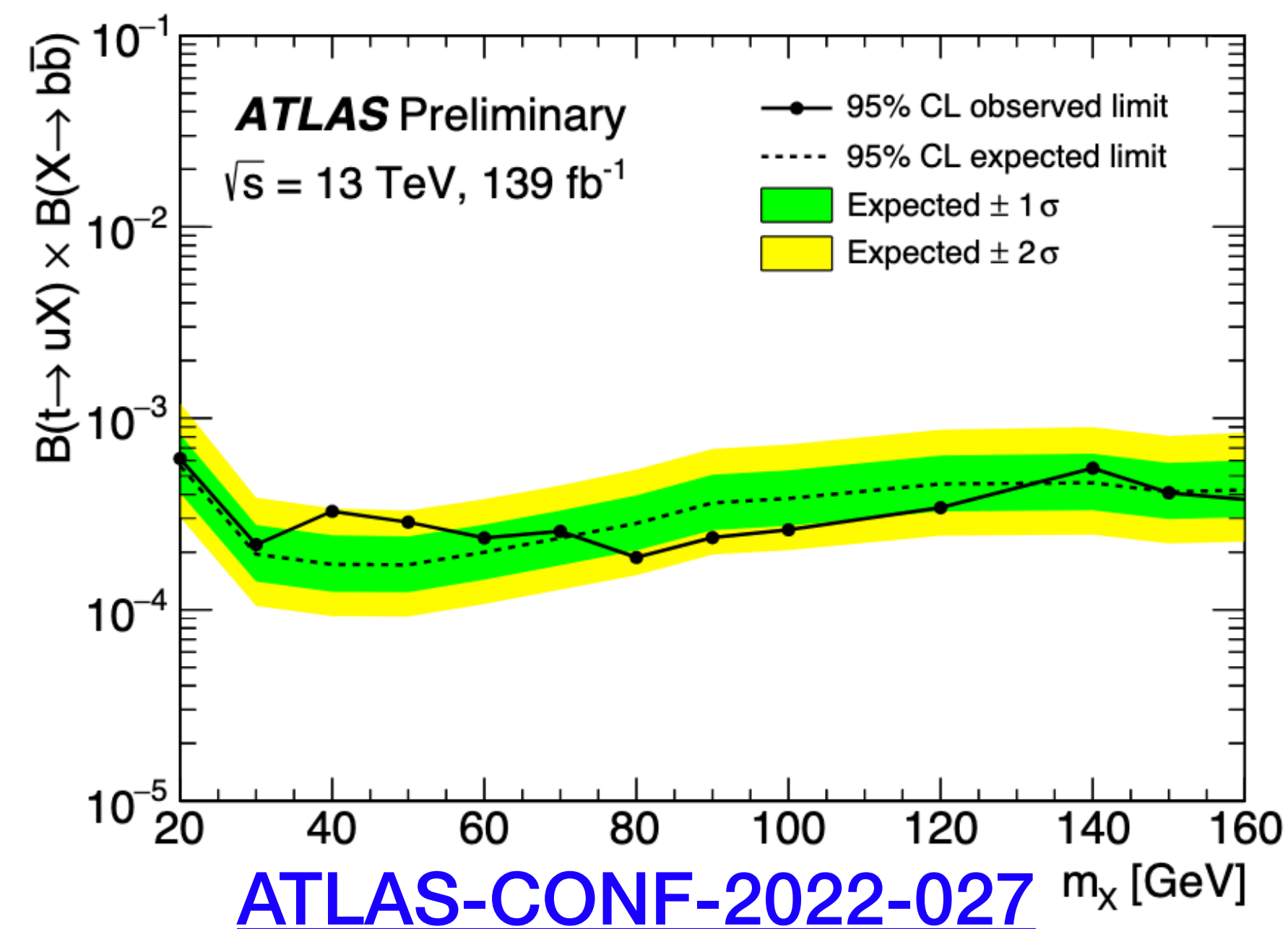
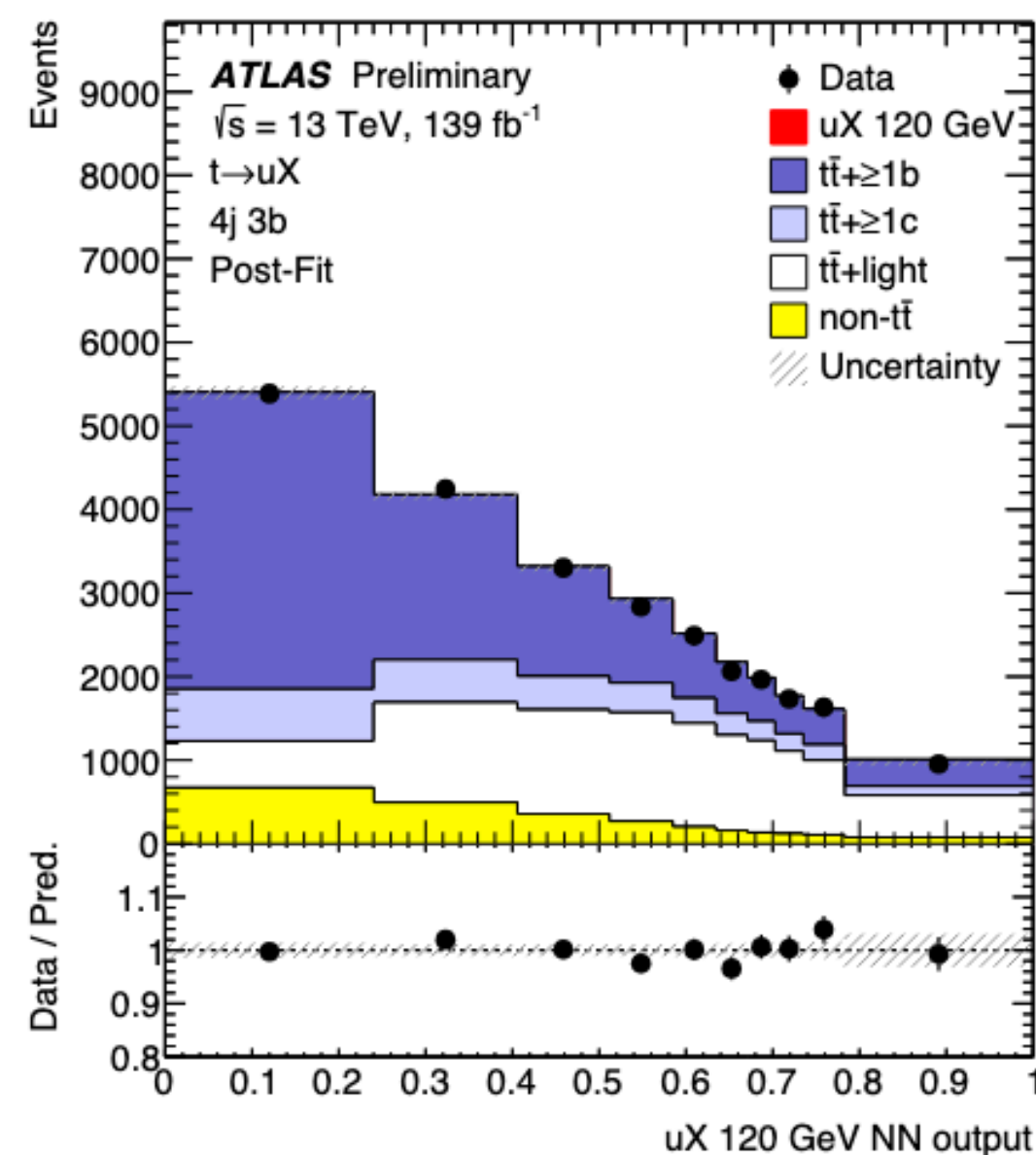
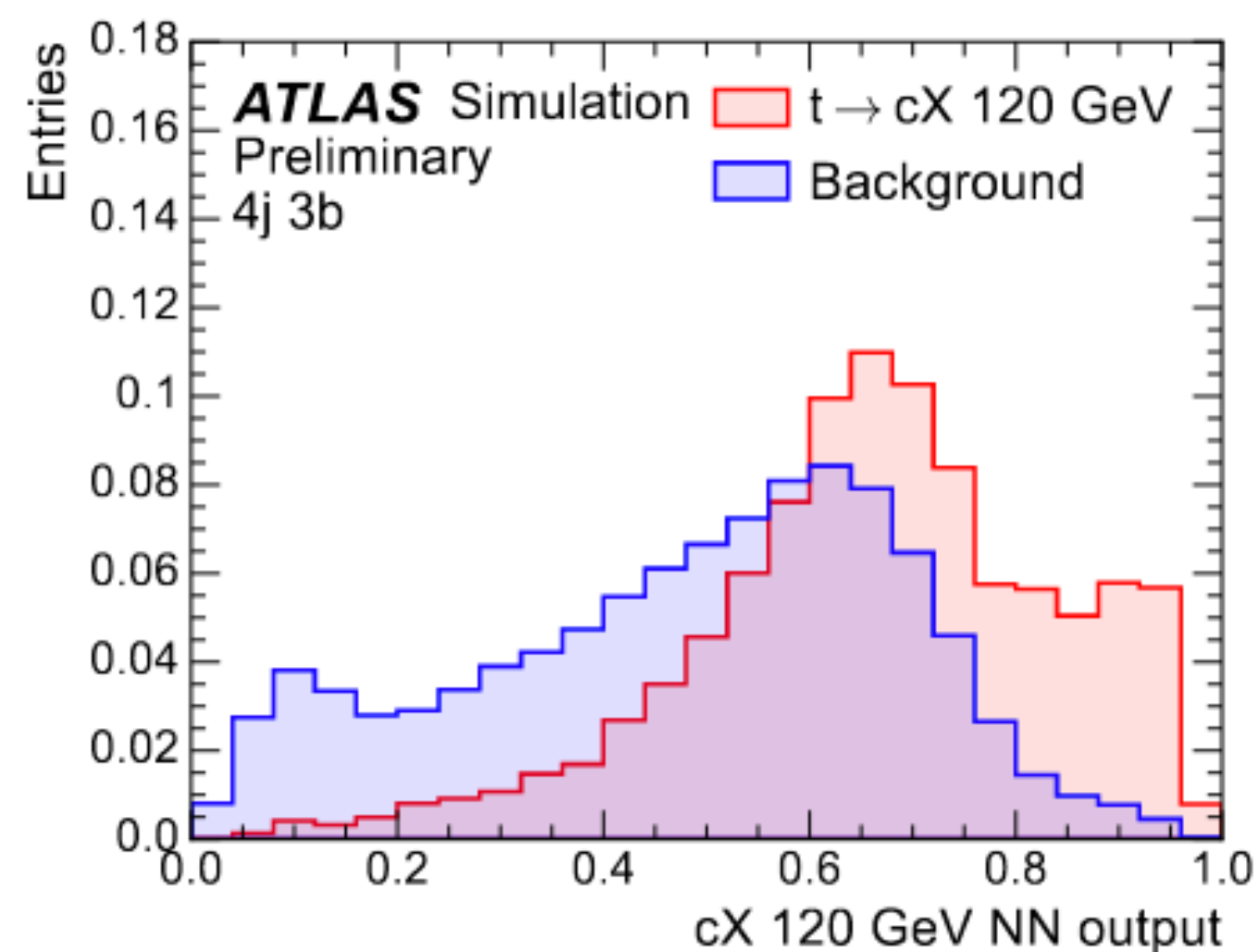
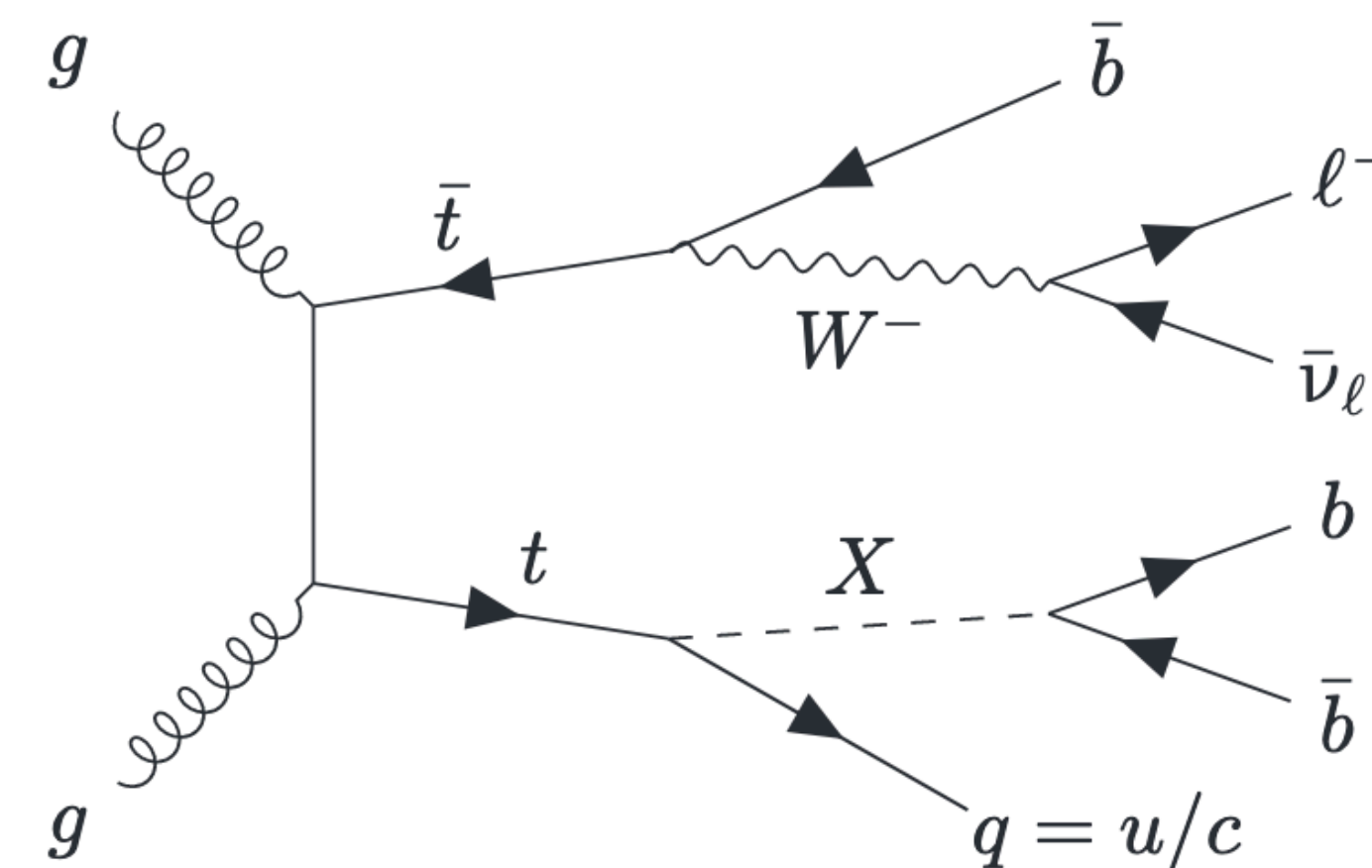
Search for scalar resonances in flavour-changing neutral currents in top quark decays

- Behaviour predicted in flavour models including light massive fields from broken approximate symmetries.

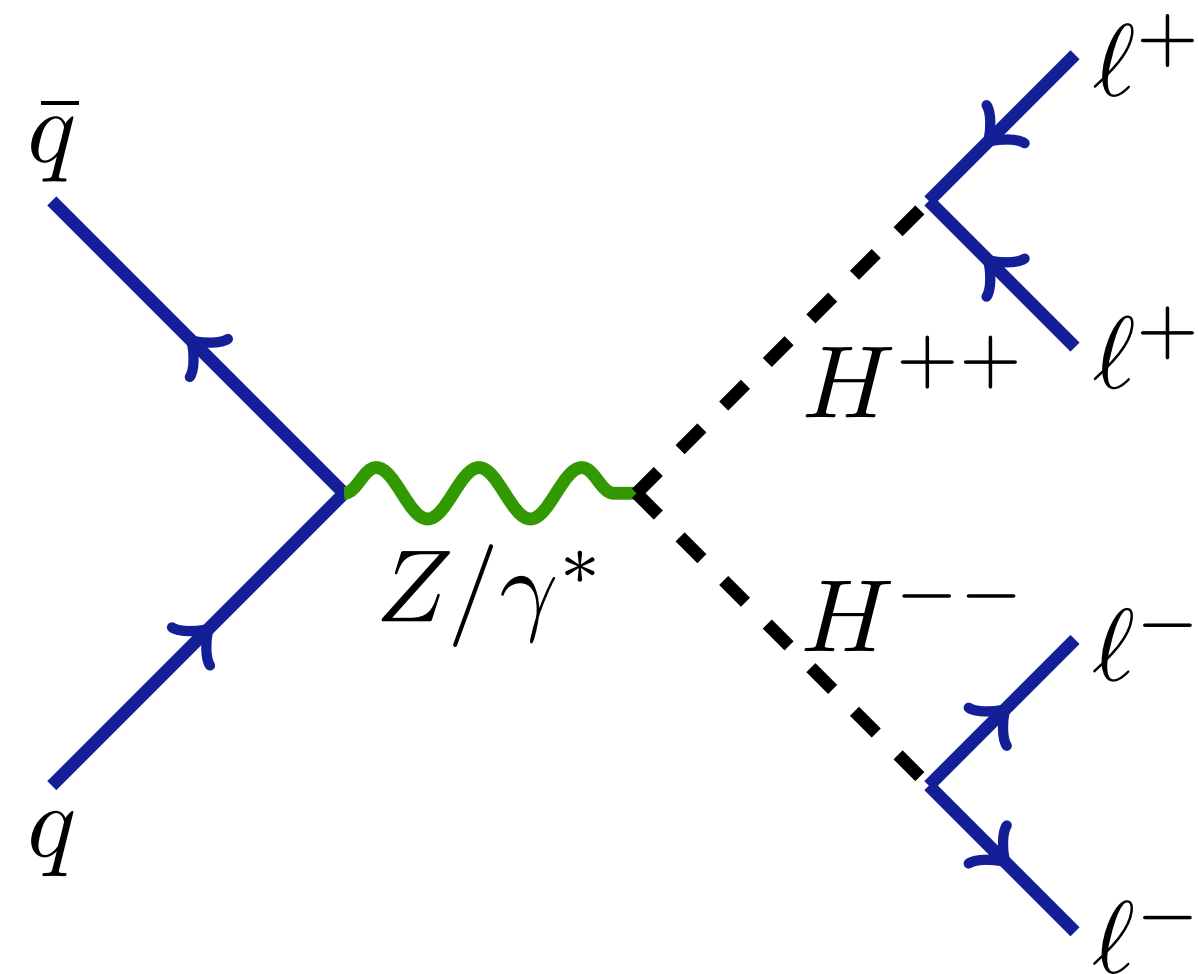
Single lepton triggers, categories defined to improve sensitivity based on the number of reconstructed jets and b-tagged jets.

- NN used for SM background discrimination

Upper limits set on $\mathcal{B}(t \rightarrow qX)$, excluding values larger than $\sim 0.08\%$.



$$H^{\pm\pm}H^{\pm\pm} \rightarrow (l^{\pm}l^{\pm})(l'^{\mp}l'^{\mp})$$



Search for a doubly charged Higgs in multi-lepton final states in the 300 GeV to 1.3 TeV mass range.

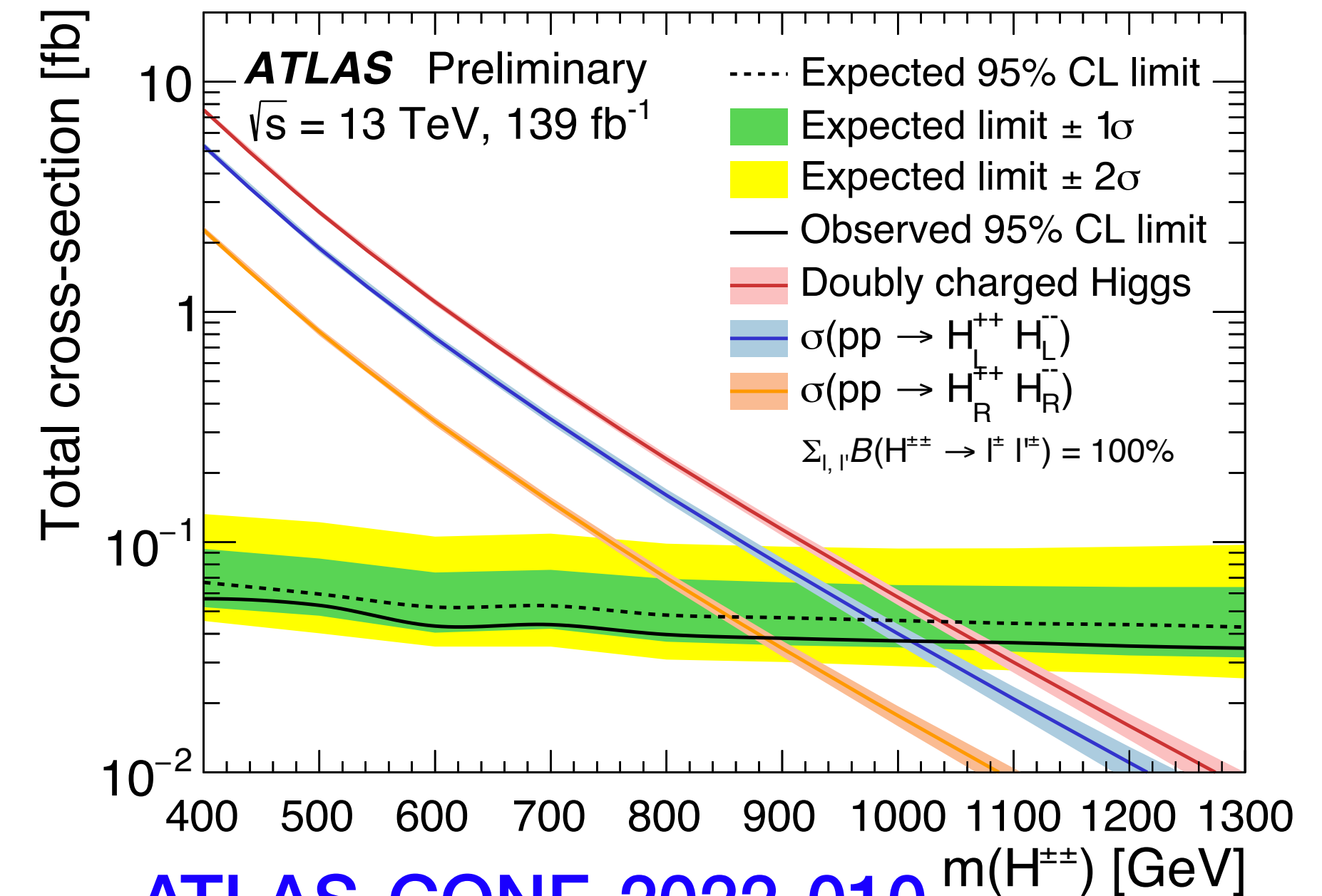
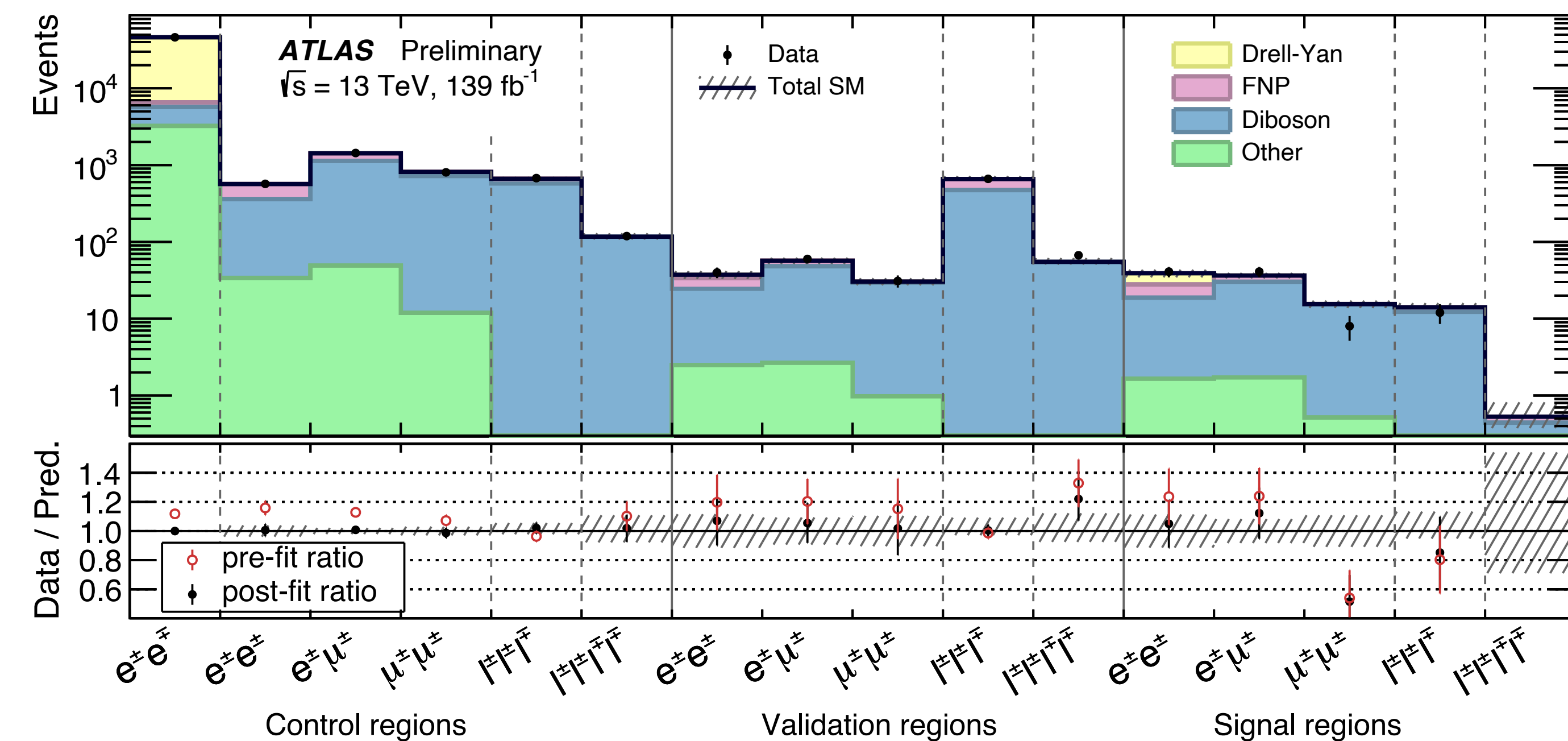
- Sensitive to lepton-flavour violation scenarios.

Data collected with dilepton triggers ($ee, \mu\mu, e\mu$)

Fit performed over the invariant mass of the leading lepton pair.

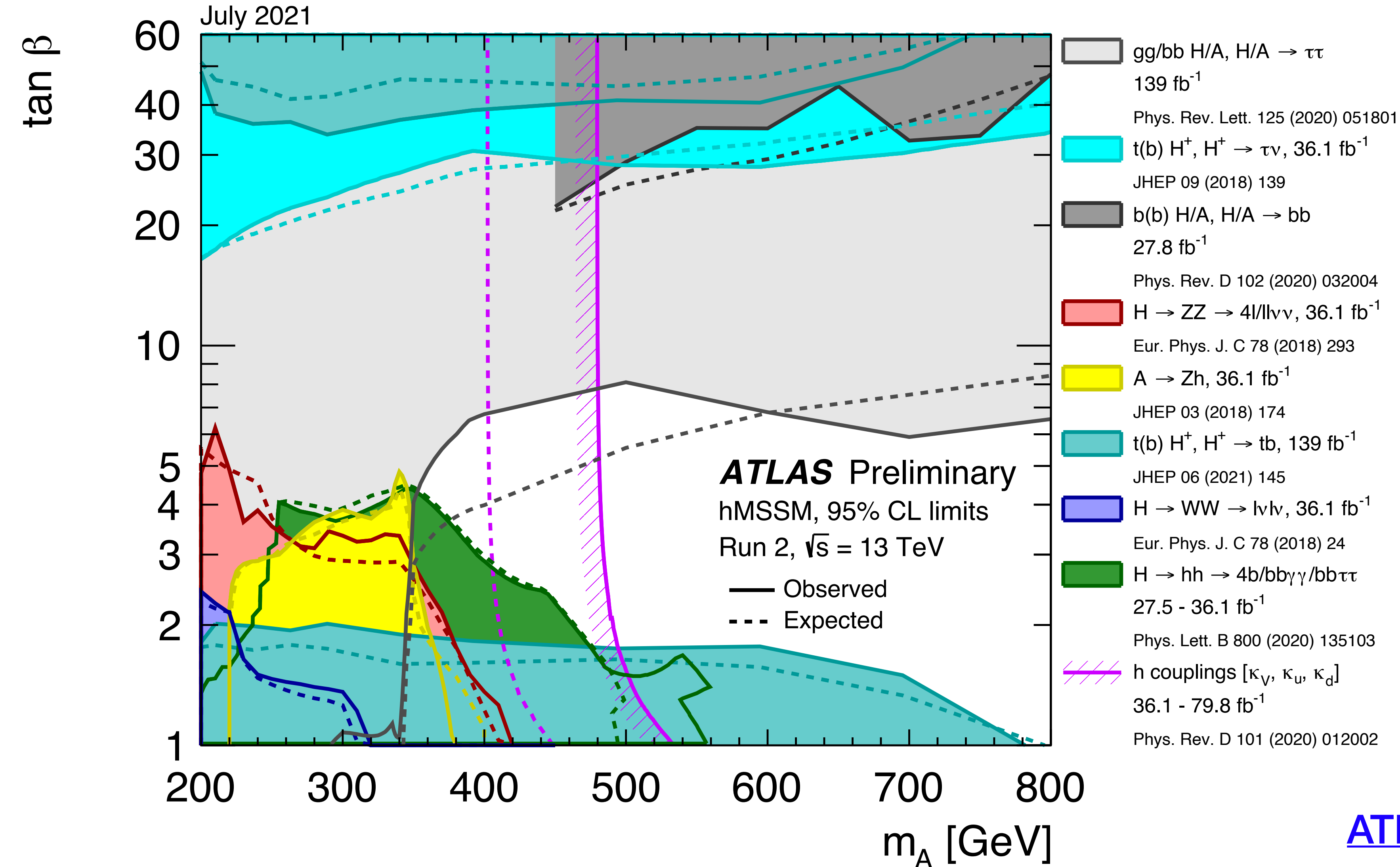
Upper limits set on the total production cross section of $H^{\pm\pm}$.

- Doubly charged Higgs excluded for masses below 1080 GeV.



[ATLAS-CONF-2022-010](#)

hMSSM summary plots from (in)direct searches



Expected and observed limits at 95% CL in the hMSSM in the $(\tan\beta, m_A)$ phase space from analyses performed at the ATLAS experiment during Run 2.

- Unless otherwise specified, only gluon fusion is considered.

[ATL-PHYS-PUB-2021-030](#)

High mass diphoton resonance search

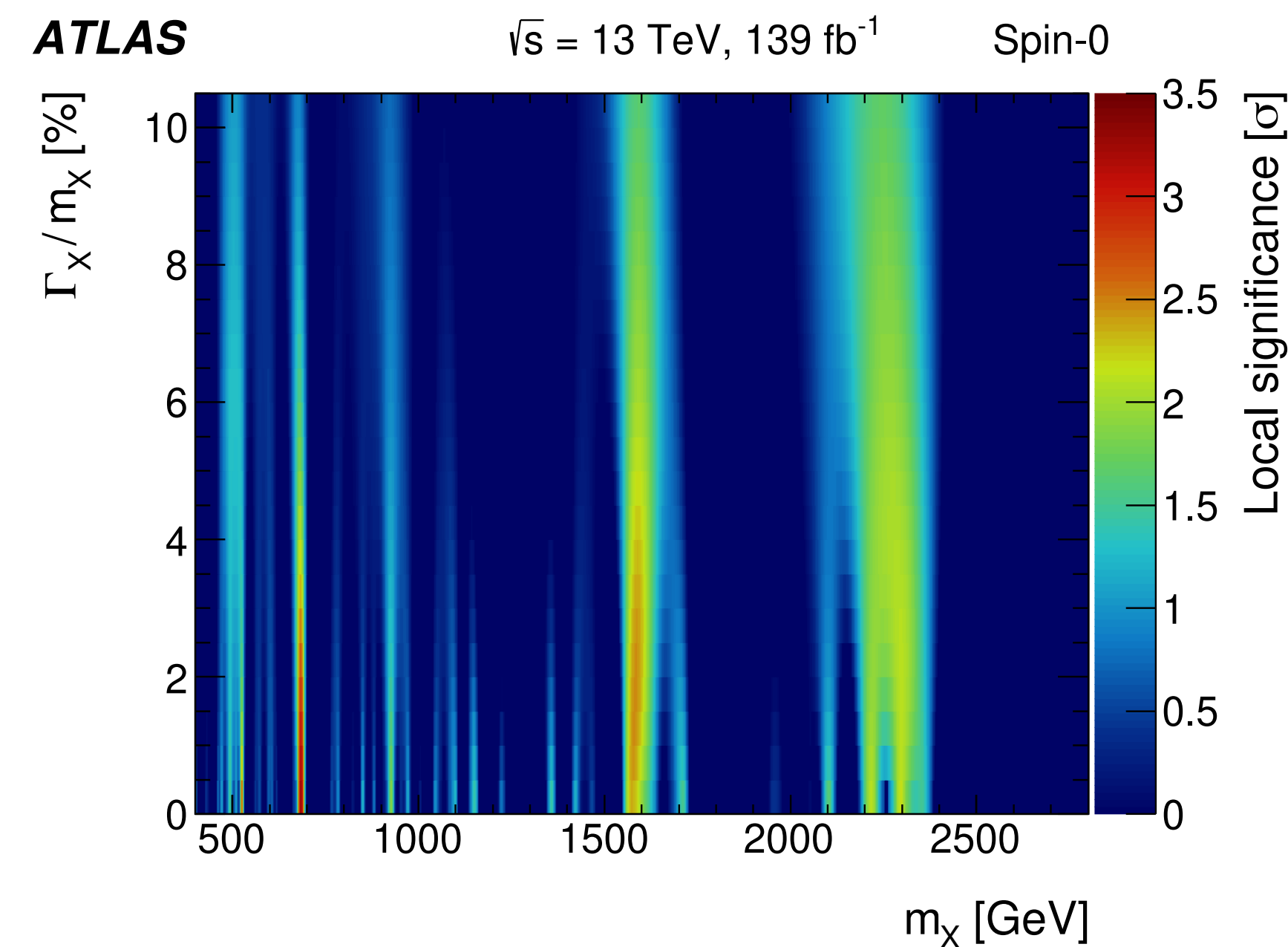
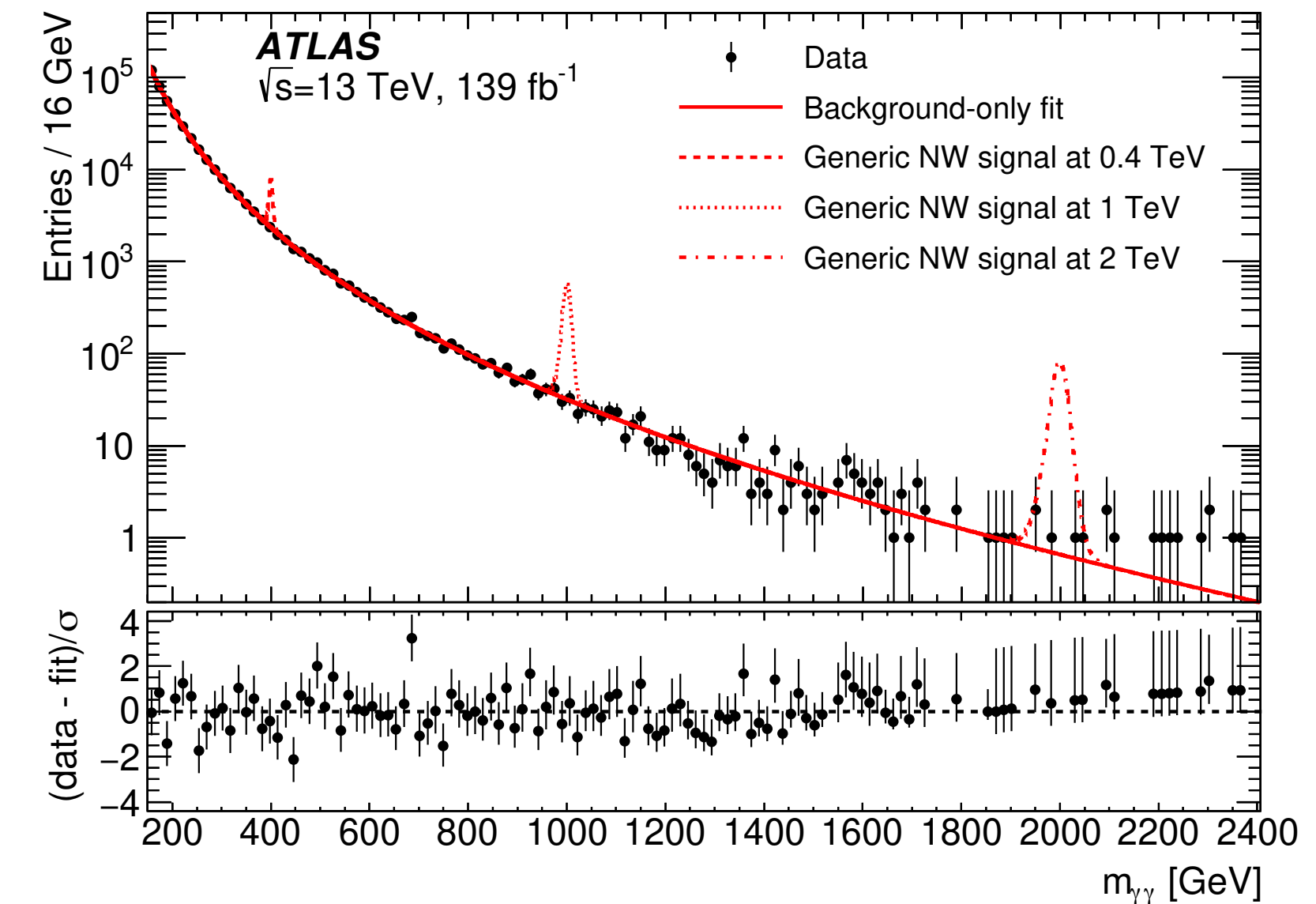
Search for high mass ($m_{\gamma\gamma} > 160$ GeV) diphoton resonances

- Benefit from excellent energy resolution and clean signature.

Signal and background shapes parametrized with analytical functions.

No significant excess observed.

- Largest excess at $m_{\chi} \sim 684$ GeV with 3.29σ (1.30σ) of local (global) significance.



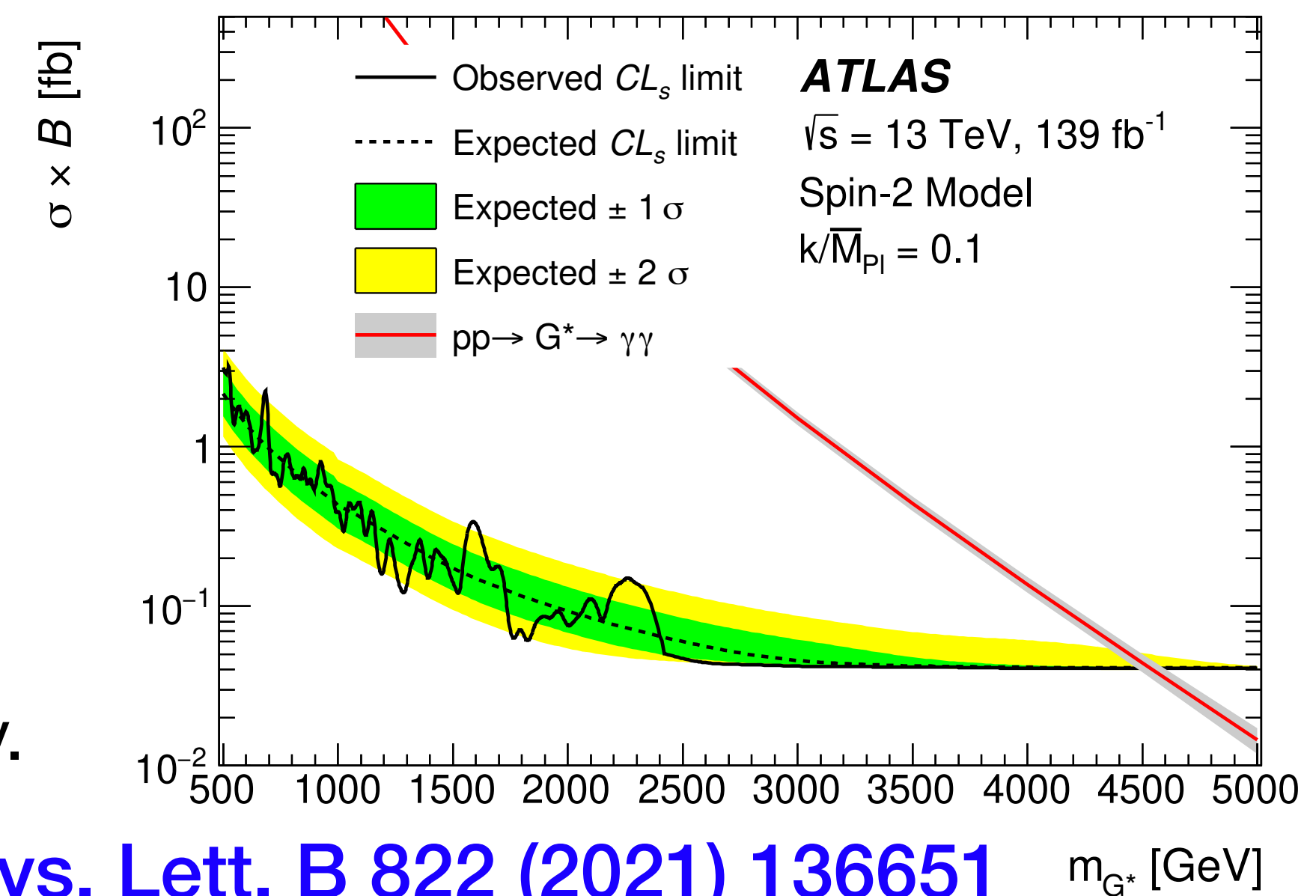
Limits are provided in a 2D plane of width (coupling) vs mass for spin-0 (spin-2) models.

Randal-Sundrum 1 model excluded for graviton masses

$$m_{G^*} < 2.2, 3.9, 4.5 \text{ TeV}$$

with couplings

$$k / \bar{M}_{Pl} = 0.01, 0.05, 0.1 \text{ respectively.}$$



[Phys. Lett. B 822 \(2021\) 136651](#)

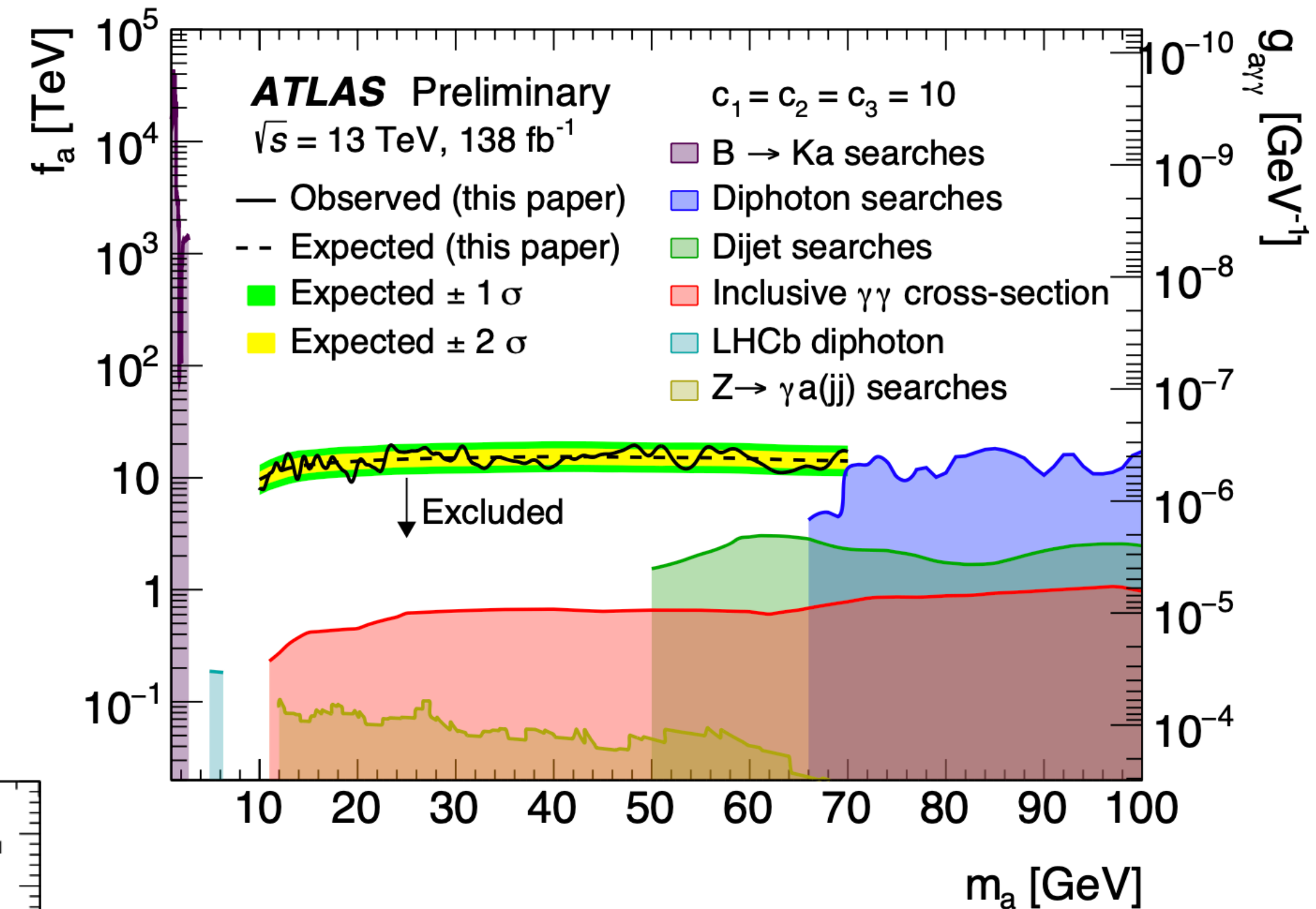
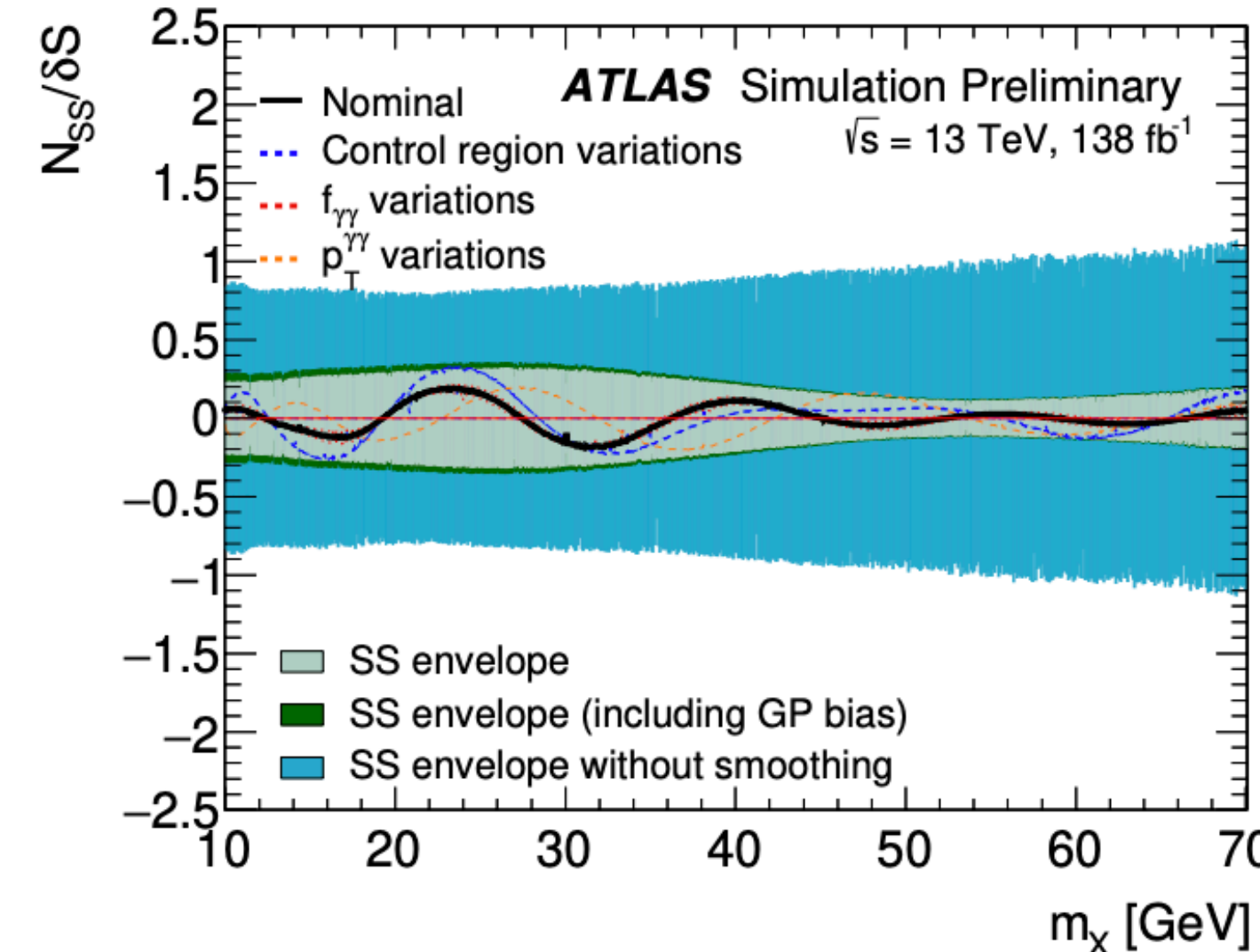
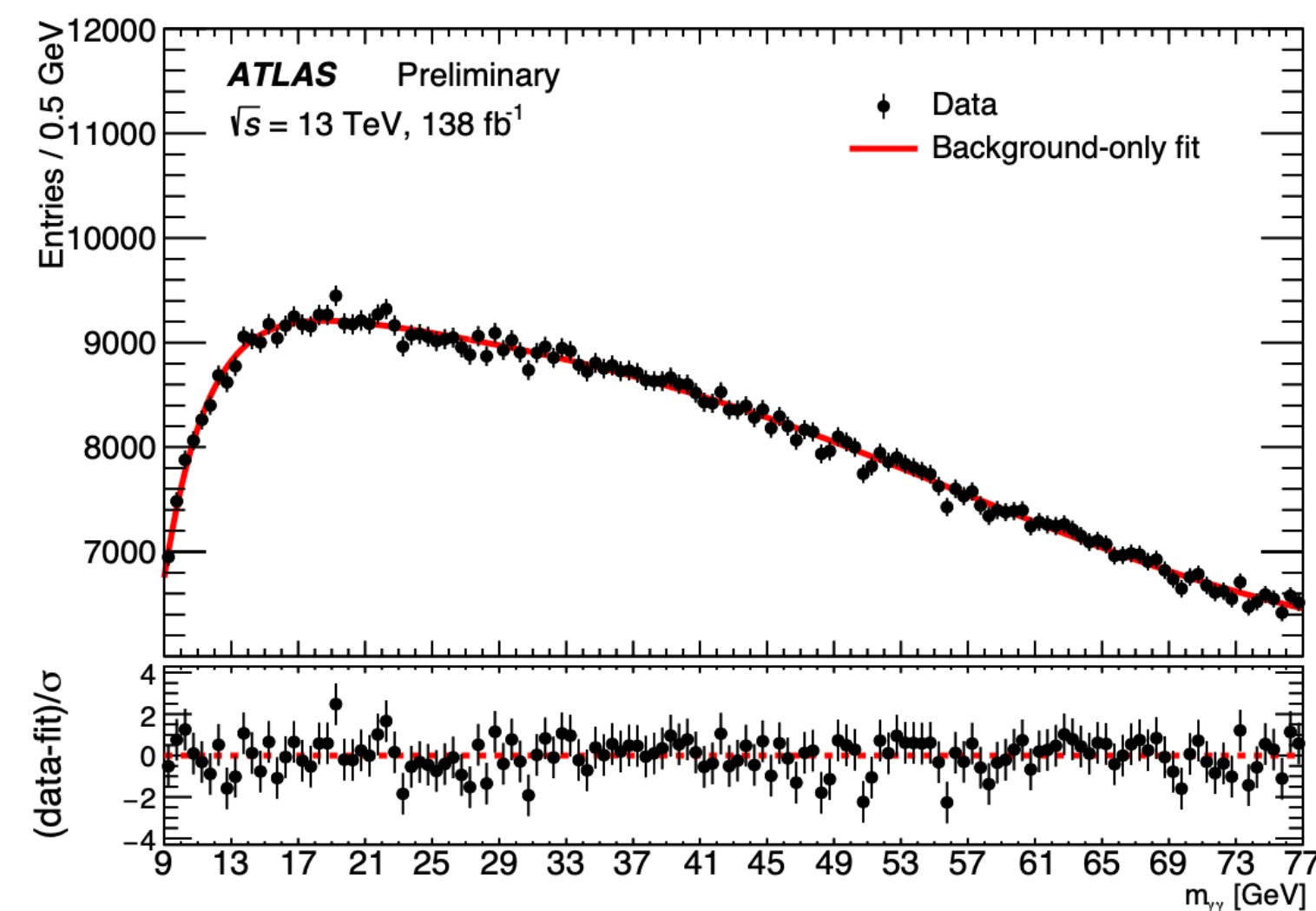
Search for boosted diphoton resonances

First LHC result with pp collisions covering diphoton masses between 10 and 70 GeV.

- Challenging background shape due to trigger sculpting the background distribution.

Selection of Lorentz-boosted photon pairs smooths background shape improving the sensitivity.

- Gaussian Process Regression used to estimate modelling systematics



No significant deviation with respect to SM prediction observed.

- Largest excess at 19 GeV, 3.1σ local (1.4σ global)
- Limits recast on the ALP parameter space

This search covers a longstanding gap in diphoton resonance searches. [ATLAS-CONF-2022-018](https://atlas.conf.cern.ch/2022/018)

Conclusions and future perspectives

Searches for additional Higgs bosons by the ATLAS experiment with data collected in 2015-2018 at $\sqrt{s} = 13$ TeV have been presented, including the production of new light and heavy resonances, and single and double charged Higgs bosons.

- No significant deviations with respect to the SM prediction have been observed.

New results released this year:

- Search for heavy additional neutral Higgs-like bosons produced in association with a pair of top quarks in the $t\bar{t}t\bar{t}$ final state.
- Search for boosted diphoton resonances
- Search for a doubly charged Higgs in multi-lepton final states.
- Search for scalar resonances in flavour-changing neutral currents in top quark decays

Work ongoing to set the machinery for the next data taking period, but interesting results are still to be published with Run 2 data.

- Stay tuned!

Backup

Diphoton resonance searches: Introduction

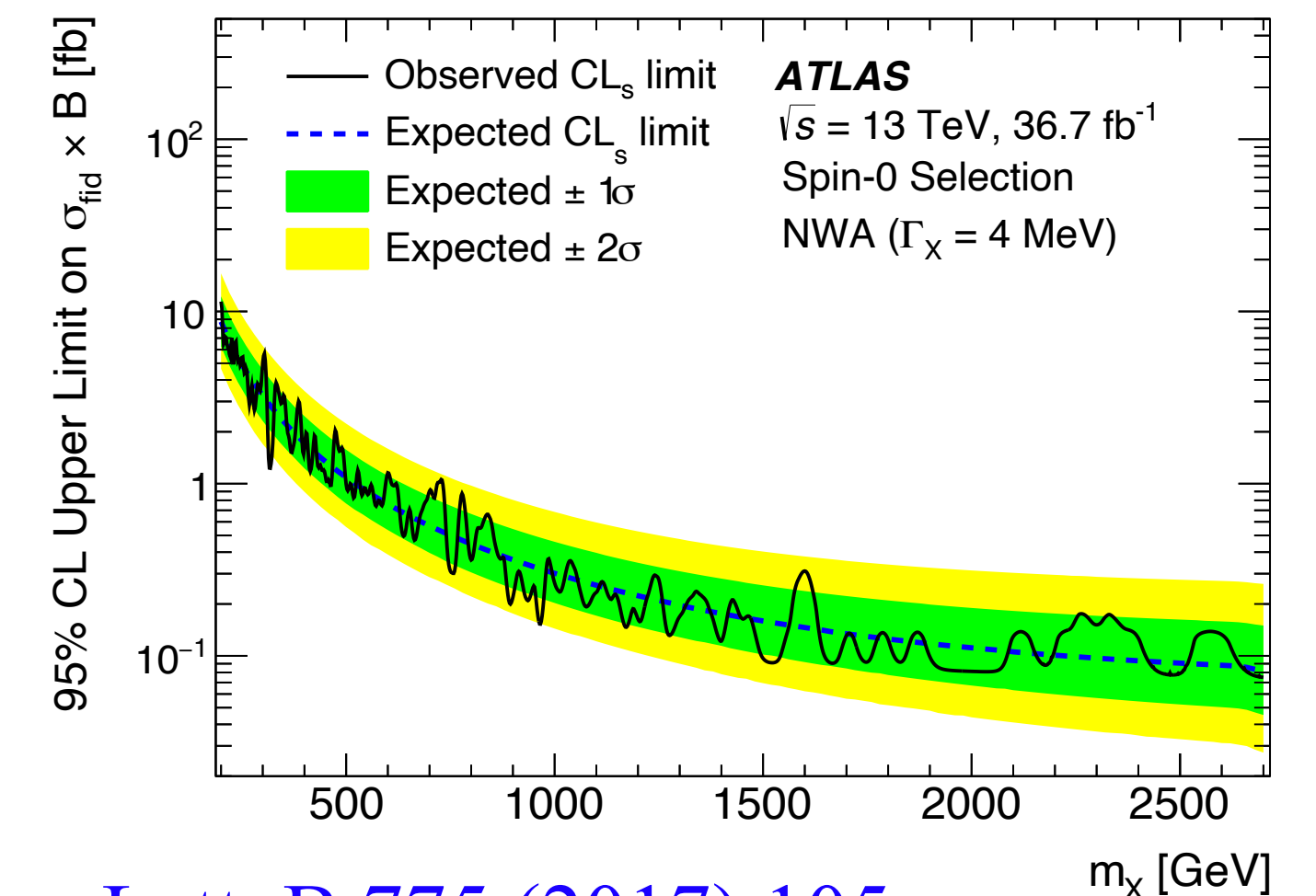
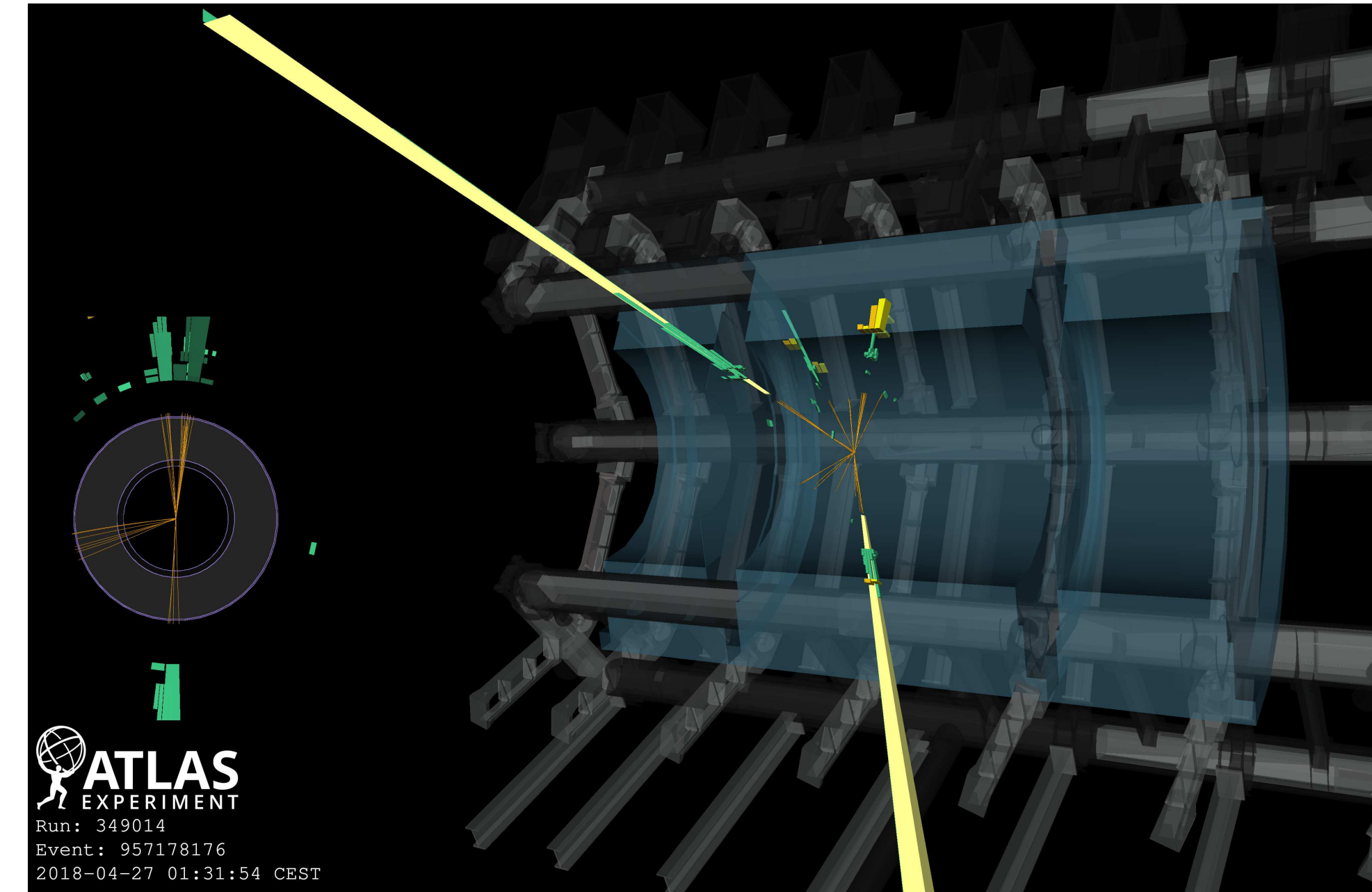
Diphoton analyses **strengths**:

- Excellent mass resolution.
- Very clean signature: 2 isolated photons in the calorimeter.

Results published with partial dataset:

- No significant excesses for diphoton invariant masses above 200 GeV.
- Upper limits expressed in terms of the fiducial cross-section to allow for easier theory interpretations.

Today: new results for the high mass range with $m_{\gamma\gamma} > 160$ GeV with the full Run 2 dataset.



[Phys. Lett. B 775 \(2017\) 105](#)

Strategy:

- Describe with analytical functions both **signal** and **background** components.
- Search for event excesses compatible with the signal shape.

Benchmark models:

- Model independent search of a spin-0 particle.
- Lowest KK graviton in the RS model: a spin-2 resonance.
 - Various widths (couplings) are considered for the spin-0 (2) search.

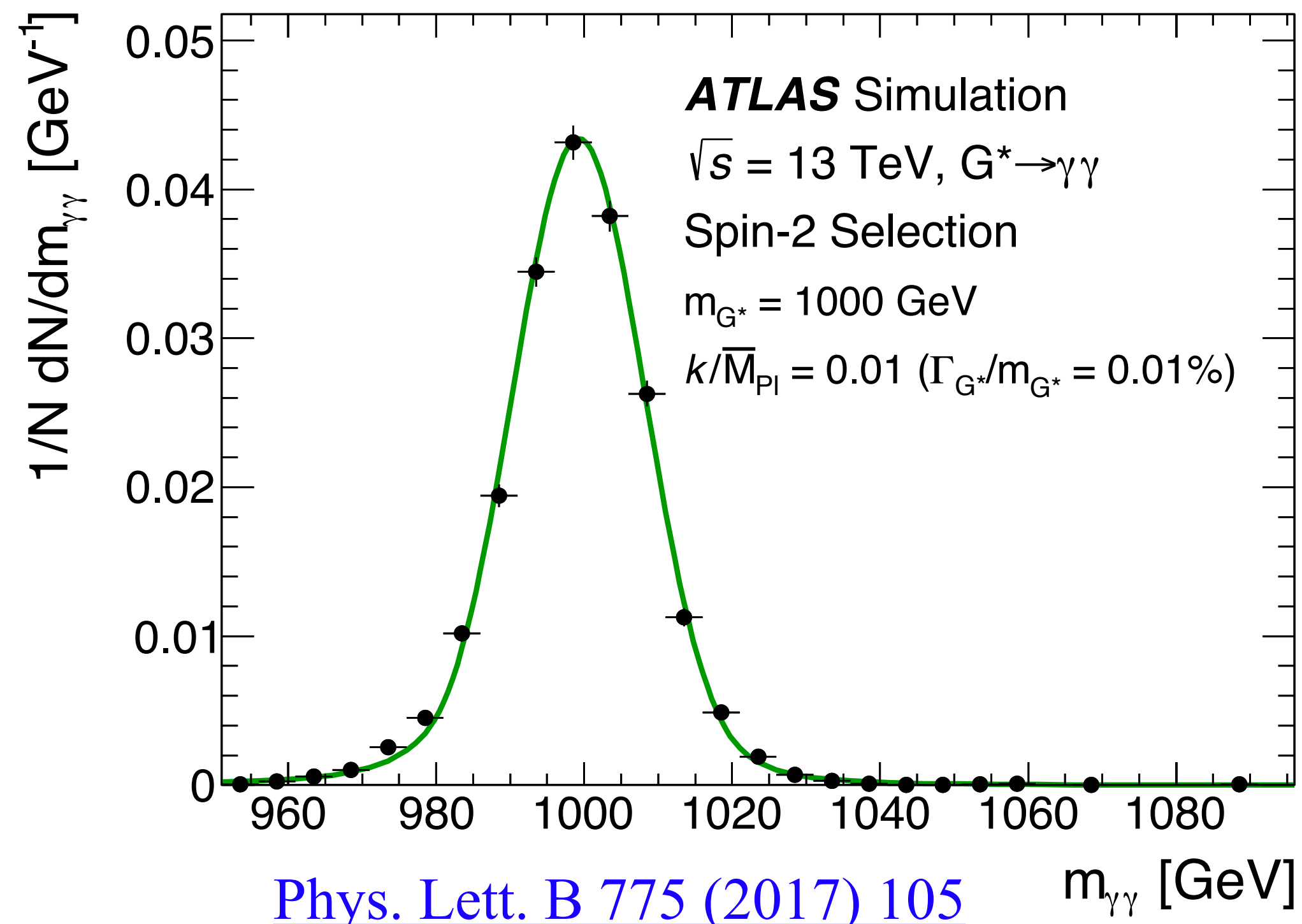
Improvements w.r.t. previous result:

- Optimized event selection common for both interpretations.
- Updated photon reconstruction, identification and calibration
- **Functional decomposition** method to reduce systematic uncertainties ([arxiv:1805.04536](https://arxiv.org/abs/1805.04536)).

Signal shape obtained from simulation.

Analytical function:

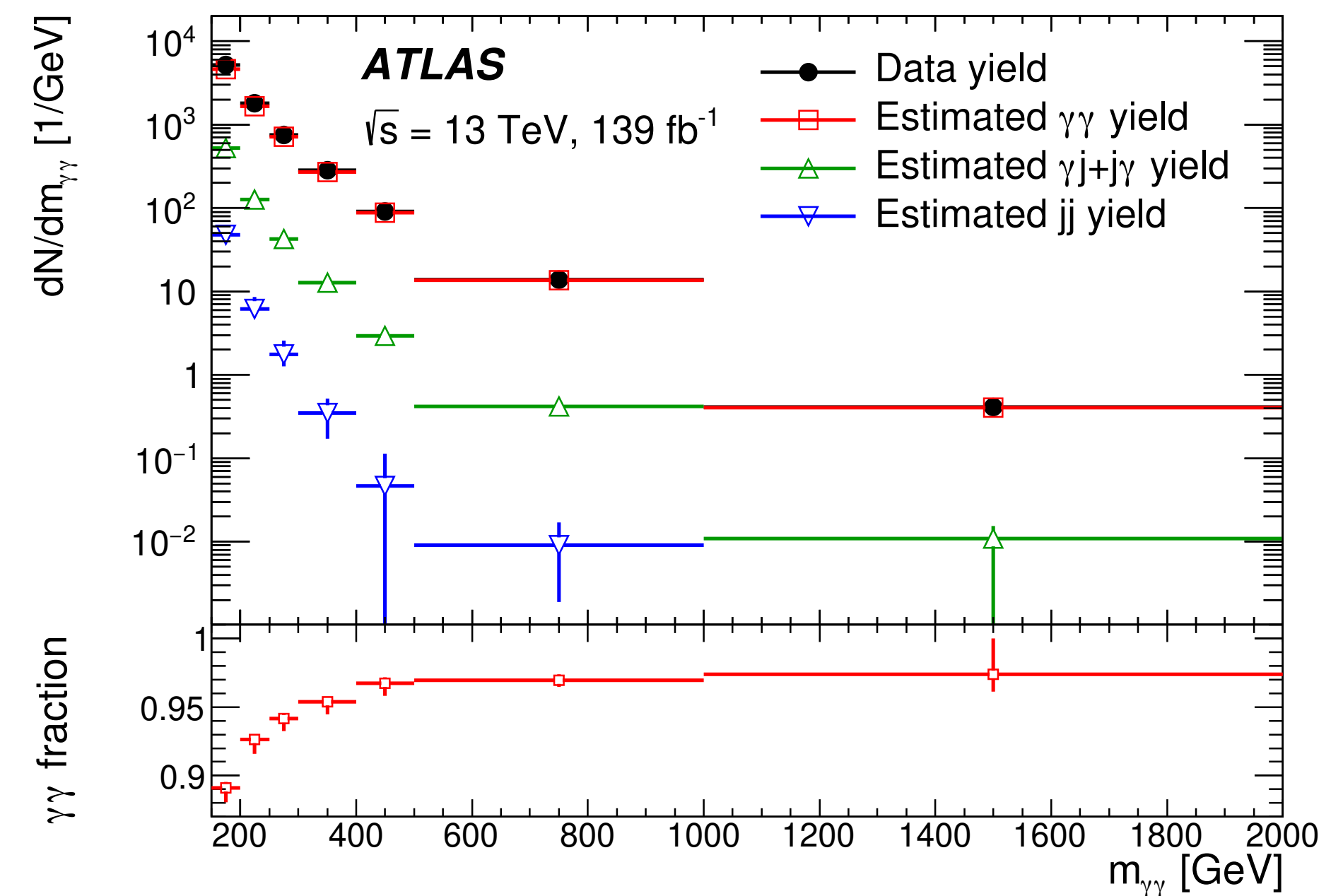
- Double Sided Crystal Ball → detector resolution
- Breit-Wigner → resonance width



Background shape obtained from simulation and data control regions.

Composition:

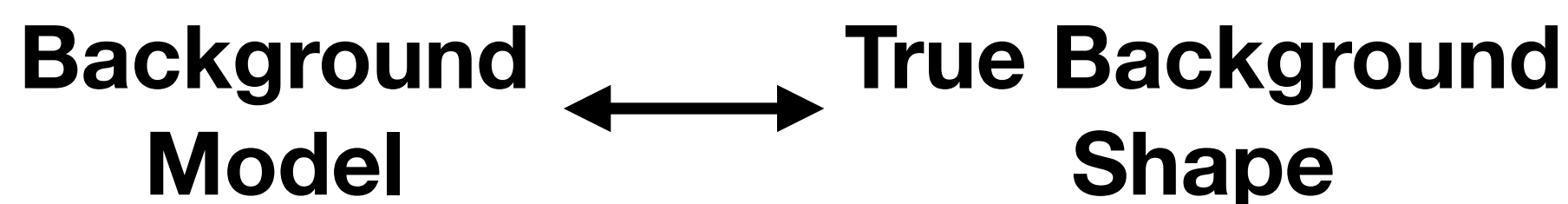
- Non-resonant QCD diphoton pairs ($\gamma\gamma$).
- Misidentified jets as photons ($\gamma j/j\gamma/jj$).



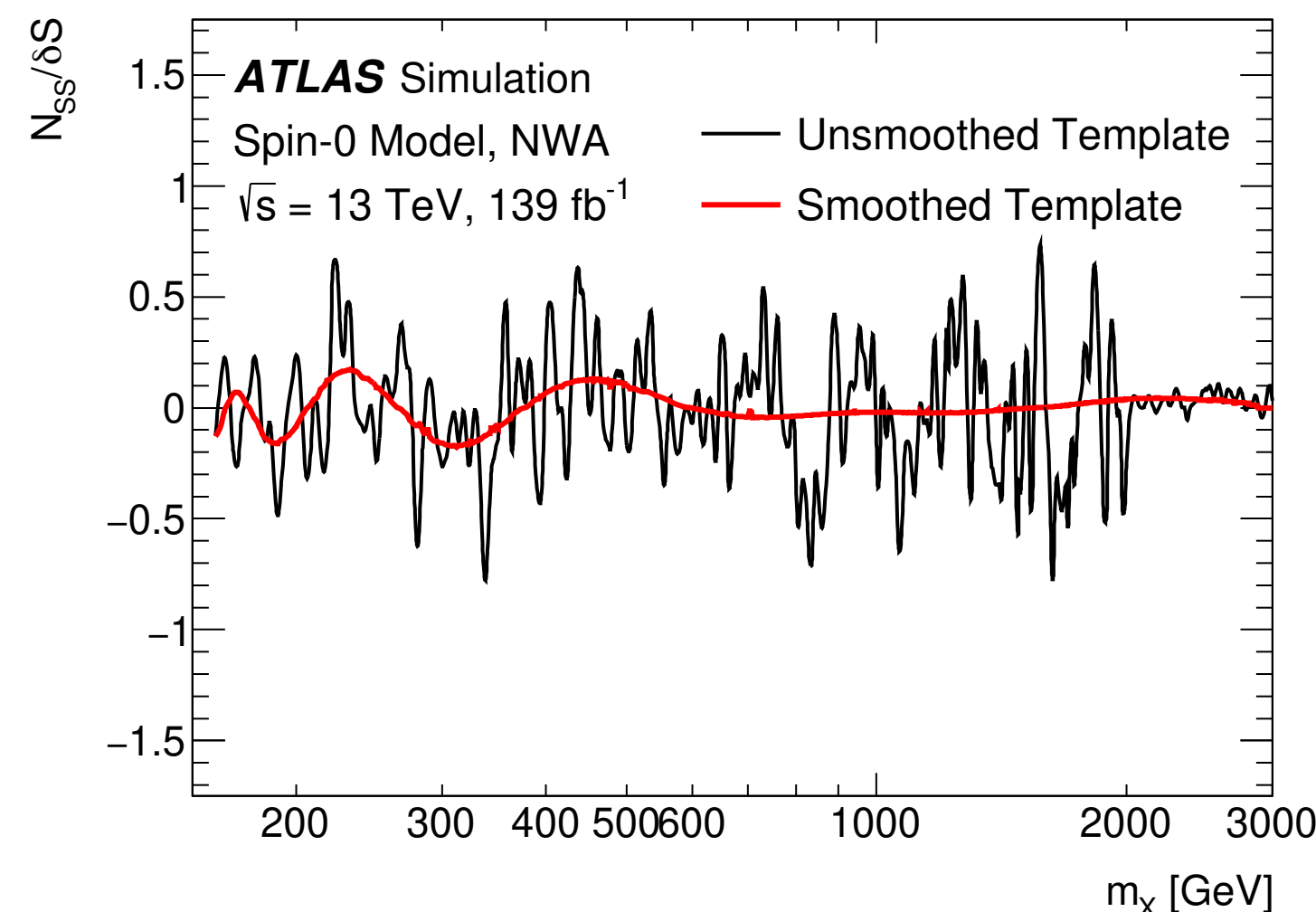
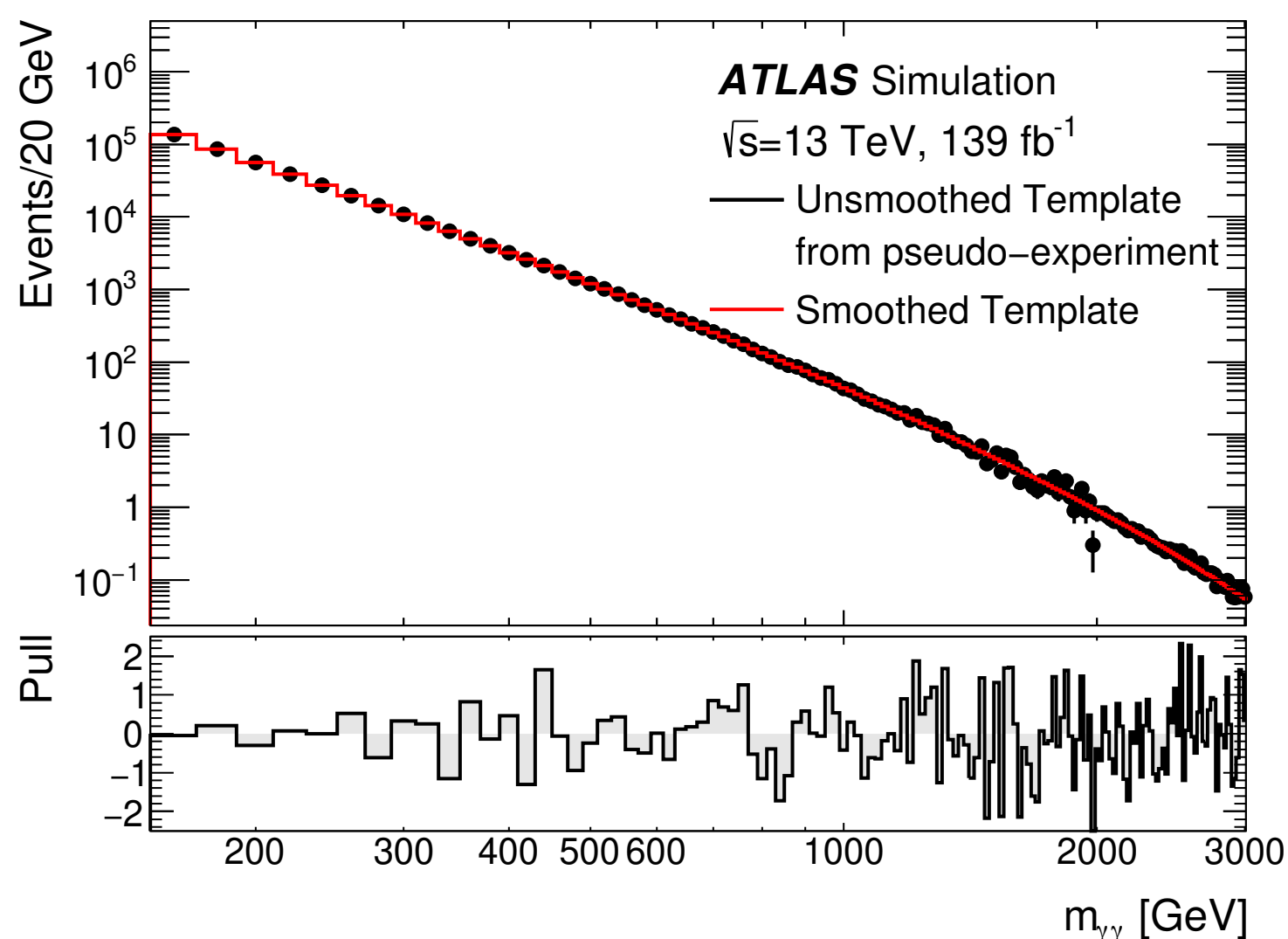
In practice, the analytic description cannot be usually derived from first principles.

- Background model empirically chosen.

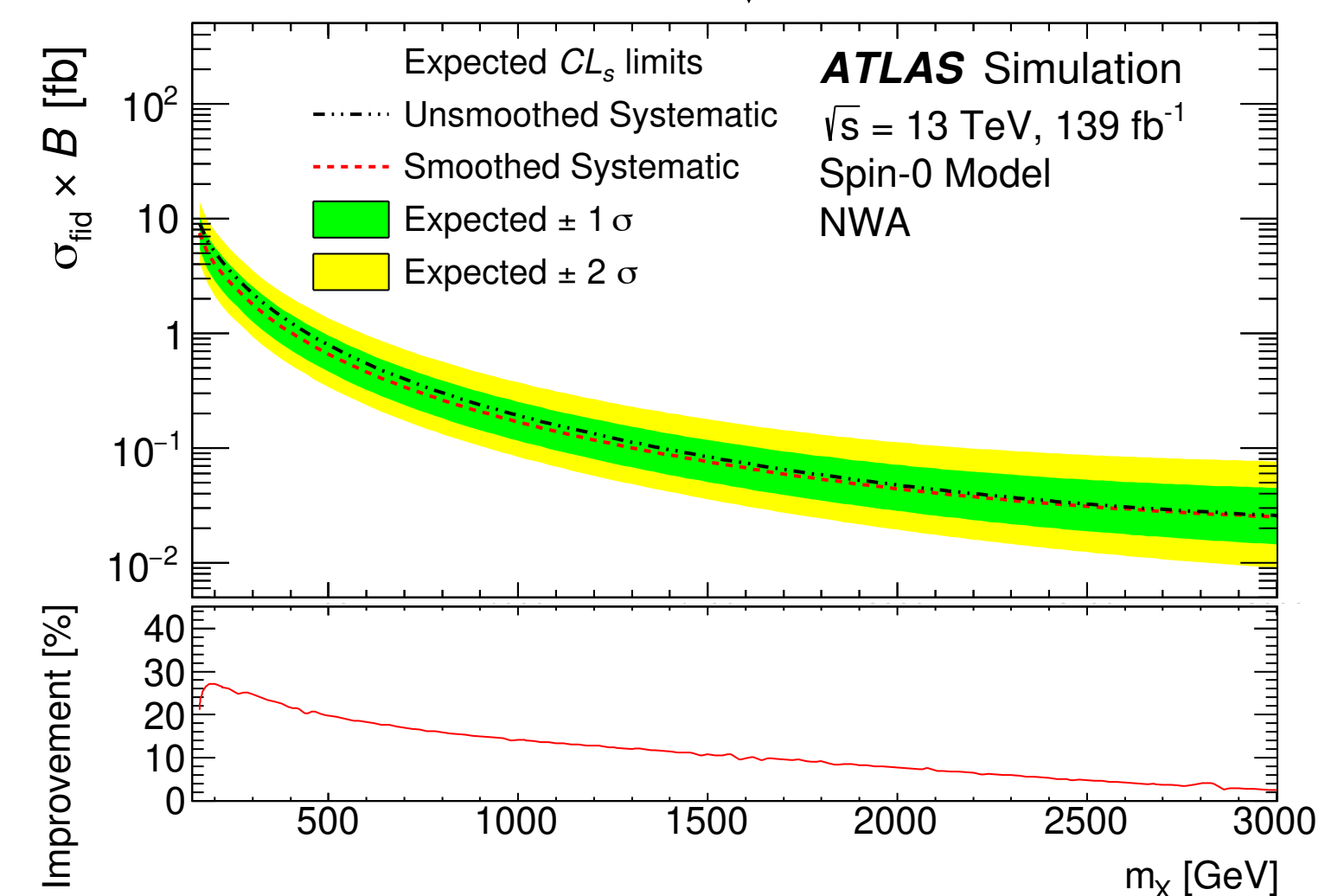
Systematic uncertainties address discrepancies between:



- A large difference could create “spurious signals” .



Improvement of up to 30% on the expected sensitivity!



Functional decomposition provides an estimate of the true background shape

Table 2: Summary of regions defined in the analysis. The table is split into four blocks: the upper block indicates the final states for each region, the second block lists the lepton multiplicity of the region, the third block indicates the mass range of the corresponding final state, and the lower block indicates the event selection criteria for the region. The application of a selection requirement is indicated by a check-mark (\checkmark), or by *inverted* when it is inverted. The three- and four-lepton regions include all lepton flavour combinations. No selection is applied when a dash is present in the corresponding cell. The average invariant mass of the two same-charge lepton pairs $\overline{M} \equiv (m_{\ell^+\ell^+} + m_{\ell^-\ell^-})/2$ is used to increase the signal significance in the four-lepton signal region.

	control regions				signal regions			validation regions		
	DYCR	DBCR2L	DBCR3L	CR4L	SR2L	SR3L	SR4L	VR2L	VR3L	VR4L
Channel	e^+e^-	$e^\pm e^\pm$ $e^\pm \mu^\pm$ $\mu^\pm \mu^\pm$	$\ell^\pm \ell^\pm \ell^\mp$	$\ell^+ \ell^+ \ell^- \ell^-$	$e^\pm e^\pm$ $e^\pm \mu^\pm$ $\mu^\pm \mu^\pm$	$\ell^\pm \ell^\pm \ell^\mp$	$\ell^+ \ell^+ \ell^- \ell^-$	$e^\pm e^\pm$ $e^\pm \mu^\pm$ $\mu^\pm \mu^\pm$	$\ell^\pm \ell^\pm \ell^\mp$	$\ell^+ \ell^+ \ell^- \ell^-$
Nr. Leptons	2	2	3	4	2	3	4	2	3	4
$m(\ell^\pm, \ell'^\mp)_{\text{lead}} [\text{GeV}]$	≥ 300	-	-	-	-	-	-	-	-	-
$m(\ell^\pm, \ell'^\pm)_{\text{lead}} [\text{GeV}]$	-	[200, 300)	≥ 300	[100, 200)	≥ 300	≥ 300	≥ 300	≥ 300	[100, 300)	[200, 300)
$p_T(\ell^\pm, \ell'^\pm)_{\text{lead}} [\text{GeV}]$	-	-	-	-	≥ 300	≥ 300	-	[200, 300)	-	-
$\Delta R(\ell^\pm, \ell'^\pm)_{\text{lead}}$	-	-	-	-	< 3.5	-	-	< 3.5	-	-
$\overline{M} [\text{GeV}]$	-	-	-	-	-	-	≥ 300	-	-	-
$E_T^{\text{miss}} [\text{GeV}]$	-	> 30	-	-	-	-	-	> 30	-	-
$ \eta(\ell, \ell') $	-	< 3.0	-	-	-	-	-	< 3.0	-	-
Z-veto	-	-	inverted	-	-	\checkmark	\checkmark	-	\checkmark	-